ADDIS ABABA UNIVERSITY
SCHOOL OF GRADUATE STUDIES
FACULTY OF SCIENCE
DEPARTMENT OF EARTH SCIENCE

DELINEATING THE OMO BASIN USING GEOPHYSICAL METHODS

By
Solomon Salih Abdu

Addis Ababa

July, 2006

DELINEATING THE OMO BASIN USING GEOPHYSICAL METHODS

BY

SOLOMON SALIH ABDU

A thesis submitted to the school of Graduate Studies of Addis Ababa University in partial fulfillment of the requirements for the Degree of Master of science in Exploration Geophysics.

July, 2006

ABSTRACT

Gravity field survey has been carried out in the Omo basin over the detail grid. The grid comprise nine, 48 km long gravity traverses, 4 km apart with gravity stations on a 1 km interval. The gravity data have been collected with the La-coste and Romberg Model G-1105 geodetic gravimeter occupation in conjunction with the post processed Fast static GPS-data acquisition using Trimble 5700.

The data were processed, analyzed and presented in contour maps and therefore are interpreted to draw conclusions in terms of basin formation.

The result shows a well-defined sedimentary basin bounded by north-south striking major structures. The Omo basin sedimentary potential has thickness of more than 3 km as deduced from the processed results, besides; its width is about15870.5 m.

In addition to its academic importance, the study will have a considerable contribution in exploring the country's hydrocarbon potential.

ACKNOWLEDGEMENTS

This thesis has been written with a number of audiences in mined, my advisor in the forefront. It is true that the intensive fieldwork, which is made possible with countless assistance of my advisor, has a great contribution to do the research.

I want to thank, Dr, Tilahun Mamo of the department of Earth science at AAU whose limitless assistance and very generous advice did very much to make this paper true. Secondly, persons who have had direct influence in doing this thesis through many days of discussion and reading were Alula Ayele, Fisseha ayele, Biruk Girma, Yohanis Gezagne. People who deserve thanks for reading and giving useful comments on the draught include; Teferi Negsh, Belay Wube, Afework Tumay.

The research work was financed through the grant from AAU. Of course, the grant extended was so meager that it would not enable this vast research project with out the assistance of my advisor. In this regard, special gratitude should go to Dr. Tilahun Mamo. More over, greater thanks must go to my mother Tiruwork Zewdie and my sister Eden Teshome for their continuous assistance in doing the research from the bening to its end.

My greatest thanks must go to my aunts Meaza and Tsigeweini Habtemariam, who used to encourage and support financially since the beginning of my education to the time this thesis become true. All the team members in field research went in to the areas of Omorate were essential in collecting the data. With out their understanding and assistance nothing would have been possible. The shortcomings are, of course, my own.

TABLE OF CONTENTS

List of figures

LIST OF TABLES

CHAPTER ONE

INTRODUCTION

1.1 Location and Access

The area of the study, the Omo basin, is located in the southwestern part of Ethiopia between 4.707249772 N - 5.014522 N latitudes and 35.839316 E - 36.282402 E longitudes (See, Fig: 5-1) that covers an area of about 1800.00 sq Kms. to the east and west sides of the Omo River. Politically the area is found in the southwest part of the southern nations and nationality and people's regional states.

A vehicle could reach the study area. It is 880kms away from Addis Ababa, riding in an asphalted road from Addis Ababa to Arba Minch and a gravel road passes through all types of weather roads from Arba Minch to konso town, and village towns of Turmi and Omorati in the south.

Within the study area, especially those in the northwestern part, there are locations that could rarely be serviced by off-road vehicles, due to the nature of the terrain, forest and infrastructural challenges. Henceforth most were accessed after the research team had looked for temporal local roads.

1.2. Objective of the study

Major objectives of the study include:

- Delineating sedimentary basins, the controlling structural boundaries and structural features.

- Mapping the structural lineaments of the area.
- Mapping the extent and estimating the thickness of the sediments contained with in the basin

1.3 Methodology

This research work was conducted based on the study of gravity field, which is originated naturally with in the earth due to gravitational sources. Thus, the gravity method of prospecting with the distinct physical and mathematical foundation, as well as data acquisition, processing and interpretation techniques was employed.

Gravity survey was carried out along the traverses laid perpendicular to the dominant directions of the geological strikes in the East-west direction across the Omo River. There, Gravity data were collected using and a La-coste and Romberg Model G-1105 geodetic gravimeter; over a grid rectangular pattern on a Km spacing to traverses of 4Kms apart.

In conjunction with the gravity survey, GPS-survey was conducted to describe, orient and reduce the gravity data. The post-processed Trimble 5700 Static-Fast static methods were performed wall at the grid station to measure GPS data. A total of 406 GPS measurement were recorded.

In processing the GPS data, Trimble GPS-survey processor software was employed. The gravity measurement report was refereed to IGSN-71 datum. Based on the aforementioned processed data, a standard component of reduction was applied to reduce the gravity values to the level of geoid. The gravity data processor was done chiefly using oasis montaj Geosoft (2003 version).

The theoretical gravity value was computed on the reference ellipsoid datum in accordance with the 1967 gravity formula.

Accordingly, the contrast between the reduced gravity observations and their corresponding theoretical values were made to obtain the gravity anomalies. Further more, the terrain corrected gravity values are filtered using methods of vertical derivative, horizontal gradient, linear and non linear spatial domain filtering. On the other hand anomaly separation was made using polynomial fitting. These gravity anomaly values are presented in contour maps.

The compiled gravity maps are analyzed and interpreted in defining the geologic structures and delineating the geometry of the study area.

1.4 Overview Of Thesis.

This thesis has been attempted to delineate the Omo Basins. It is comprised of seven chapters. The first chapter deals with the introductory part of the study. The second chapter includes the geological and physical review of the area under study. The theoretical aspect that provides ground for the research on the basin is discussed in the third chapter.

Descriptions on GPS survey data acquisition together with the ground for the final processed and adjusted results are presented in chapter four. The fifth chapter consisted of the field gravity data acquisition, and determination of the Omo Basin gravity value referenced to IGSN-71 datum. The sixth chapter is devoted to the compilation, presentation and interpretation of the gravity data. Conclusions and recommendations are presented in last chapter.

CHAPTER TWO

GEOLOGICAL AND GEOPHYSICAL REVIEW

2.1 The Regional Rift Basins and Sedimentation

Jurassic to Early Tertiary rift tectonics in east Africa resulted in developing a large system of rifts that extends from northern central Sudan to southeast Kenya. These have been collectively known as the Central Africa Rift System. The southern Sudan rift basins are, in most cases, believed to have connection with the Anza trough of Kenya along E-W striking zone at about northern part of Lake Turkana or the southern end of the OmoBasin.In the south OmoBasin, these Central African rift segments join at an angle of 45° with the Neogene East African rifts,and the likely presence of Mesozoic. Early tertiary sediments underneath the Neogene Omo-Turkana rift sediments has been suggested in several studies. Since information is scanty and/or as no significant geological and geophysical have been done yet at the area of the junction of the two rift systems, satisfactory account cannot be given regarding basins geometries and the sedimentary sequences in these basins. However it appears worthwhile to have some knowledge about the general outline of the basins and the sedimentary units where enough data is available. In this regard the Sudan rift basins and the Anza basin of Kenya that have been studied by oil companies and academics since long time ago could serve in providing information relevant to the general geo-tectonic setting and the sedimentary history.

2.2. The Omo Basin and its Regional Settings

The southern rift basins, Omo and Chew Bahir basins, form part of the active Neogene-Recent East African Rift system. The two basins are separated by broad, uplifted Precambrian terrain of the Hamer plateau and branch out to the north in to several troughs and grabens known by separate names .all these rift basins along with the Omo and Chew Bahir collectively, constitute what is generally known as the Broadly Rifted Zone of south –western Ethiopia. The OmoBasin (the east) is the northern extension of the Turkana Rift. Whereas, the Chew Bahir is the northward extension of the Kenya Rift. The Main Ethiopian Rift, with a general NE-trending axis lies about 200 Km to the NE of the Omo rift. Multiple extension, rifting and volcanism occurred since the mid-Miocene to the quaternary in these rifts (in the broadly rifted south western and Main Ethiopian rifts). The amount of extension, the geometries of the basins and the sedimentary infill history of these rift basins are not well understood yet.

2.3. Recommendations

The Omo Basin appears to bounded by N-S- striking major fault segments and bifurcates to the north in to Mago and west Omo sub basin. The basin is suggested to have a westward-tilting configuration (Ebinger,et.al,1993).Up lif of the Hamer plateau and westward- tilted Oligocene and Pliocene basalts in the eastern part of the basin are suggested as indicative of the westward tilt of the Omo Basin in the Neogene time. According to Ebinger, et.al,(1993), about 100meter section has been removed by erosion on its Eastern margin.

Several studies undertaken in the Omo-Turkana basin have indicated that Paleogene volcanic units along the margins are also interbedded with thin fluvial sedimentary units, and Fejej basalt (Oligocene) in the eastern side of the basin is reported to contain interbedded fluvial sediments within its thick, about 100 meters section. Moreover, lacusrtine sediments of Lower Miocene age (which are inerbedded with tuffs) lie above the Fejej basalts along the eastern part of Lake Turkana. Volcanic and sedimentary strata overlapping the Oligocene basalts at the margins along the western side of Lake Turkana are indicated by seismic reflection data. The volcanic-sedimentary section in this western part of the basin, beneath Lake Turkana is estimated as more than 4 Km, thick.

Based on gravity data acquired over large part of the East African region (including the Omo and Chew Bahir) models forwarded by Ebinger et.al.(1993) indicate the presence of cretaceous sedimentary strata estimated more than 1Km in thickness in the eastern margin of Lake Turkana. The models are constrained by seismic data (refraction and reflection) from northern Lake Turkana area and from geological structural data and topographic studies made over large part of the region. Seismic and subsidence modeling studies along the length of Kenya rift also have shown that crustal thinning underneath the Turkana area gets more pronounced as compared to the rifted zone in the south. The increased crustal thinning towards north along the length of the Kenya rift is suggested to have been attributed to, perhaps, superposition of the rifting events from the Jurassic through recent time in the omo (north Turkana) rift basin region. Based on geological and geophysical data the link between the Muglad and Anza rift basins along E-W striking faults has been suggested in several studies Tthis link is in the vicinity of the Omo Basin and it indicates that the Anza rift probably continues northwest beneath the Omo rift.

CHAPTER THREE

THE GRAVITY SURVEY METHOD

3.1 The Method In General

The physical property variations of rocks in -situ must be related to a greater or lesser extent to what we loosely term the 'geology' of the subsurface (Petrson, J.C. And C.V. Reeves, 1985).

Gravity Method involves the measurement of changes in the gravity field of the earth. This is a natural source method in which local changes in density of rocks in -situ given rise to minute changes in the gravity field of the earth that may be measured at and /or above the earth's surface and in fact-under ground measurements have also been carried out occasionally.

The Gravity Method attempts to measure small differences in force of the gravity field which is relatively huge. The gravity field varies with position and to lesser extent with time. In this method it is possible to determine the absolute gravity field.

The earth's surface does not represent a regularized equilibrium surface and therefore, the measured gravity values vary in accordance with the variations in latitude, elevation, topography of the surrounding terrain, earth tides and subsurface density changes.

Hence, gravity values are reduced to an equipotential datum applying the appropriate components of gravity reduction to compute the different gravity anomalies. The anomalies yield information about the changes of density with in the earth as well as about the surfaces that bound regions of differing density. The information is, however, always subject

to certain fundamental ambiguities inherent in the theory of the Newtonian potential.
Moreover, anomaly separation and wavelength filtering may be necessitated to reveal a better picture of the subsurface.

The method is popularity used to investigate geologic structures which is represented by density contrast with out the need to touch, see, or disturb the rock itself.

Although expensive it is considerable cheaper than the seismic method and therefore are employed in the forefront in oil exploration.
In fact-no other methods can tell as so much so little cost i. e relatively .The continuing demand for gravity data around the world is ample evidence for this (Telford, 1980).

3.2 Fundamentals Of Gravity

3.2.1. Force Of Gravity

Newton's universal law of gravitation is the basis for gravity work. This law relates a mutual force **F** of attraction between two point masses to their respective masses, m_1 and m_2 and the separation **r** between them:

$$\mathbf{F} = -G\,(m_1 m_2/\mathbf{r}^2)\,\mathbf{e_r} \qquad (3.1)$$

Where,
$\mathbf{e_r}$ is a unit vector directed from m_1 towards m_2, conveniently, when F is the force acting on m_2;
G is the universal gravitation constant which has a measured value of 6.612x10E-11 Nm^2/Kg^2 in SI units.
The negative sign arises because the force **F** is always attractive. Note that Equation (3.1) Newton's law of gravitation originally holds for point masses are applied to find the gravitational force **F** between a sphere of a

uniform concentric shell structure and a point mass located to the sphere.

3.2.2 Earth's Force of Gravity

If the earth is made up of homogeneous spherical shells that did not rotate, i.e., when the effects of rotation and non-uniformity of the sphere and density is neglected as if it where a sphere of uniform concentric shell structure, the force of gravity **F** exerted by the earth's mass M_E on a point mass m located on its surface can be found from Equation (3.1) as :

$$\mathbf{F} = (G\, M_E\, m/\mathbf{R_E}^2)\, \mathbf{e}_r \qquad (3.2)$$

Where,

- **F** force of gravity
- M_E the earth's mass
- $\mathbf{R_E}$ the earth's radius
- m a point mass on Earth's surface
- G Universal gravitational constant, G=6.612x10E-11Nm^2/Kg^2 in SI units and,
- $\mathbf{e}_r$ a unit vector directed from m toward the earth's center along the radius

3.2.3 Earth's Acceleration of Gravity

Returning to Equation 4.2 the acceleration of gravity g of m due to the presence of M_E can be determined by dividing **F** by m. Thus, the acceleration of gravity of m at the surface of the earth is:

$$\mathbf{g} = \mathbf{F}/m = G\, M_E\, /\mathbf{R_E}^2)\, \mathbf{e}_r \qquad (3.3)$$

Where $\mathbf{e}_r$ is a unit vector towards the center of the earth along the radius**.**

Units for Gravity

The SI unit for gravity **g** is m/s^2. In geodesy and geophysics the auxiliary unit milli Gal (m gal) is often used.

Thus, units of **g** and conversions

$1\ cm/s^2 = 1$ gal

$1\ m/s^2 = 10^2$ Gal$=10^5$ m gal $=1$g.u.

.

3.2.4 The Gravity Potential

The analysis of certain kinds of force field can be simplified using the concept of potential. The gravity potential, U, at a point is defined with in earth's gravity field as the work done by the force of gravity in moving a unit mass from an arbitrary reference point usually from infinite distance to a point a distance **R** from the center of gravity of M. Thus, the gravity potential, U, is given by:

$$U(\mathbf{r}) = G\,M \int d\mathbf{r}/\mathbf{r}^2$$

$$U = GM/R \qquad (3.4)$$

The force of gravity giving rise to a conservative field may be found from scalar potential.

$$\nabla U(\mathbf{r}) = \mathbf{F}(\mathbf{r})/m = \mathbf{g}(\mathbf{r})$$

(3.5)

Alternatively the gravity potential can be derived in the form.

$$U(\mathbf{r}) = \int g.dr = -GM \int dr/r^2 = GM/R \qquad (3.6)$$

This is equivalent to Equation (3.4)

The gravity g is pertinently found from Equation (3.5), i.e., the gravitational acceleration along the force is defined as:

$$\mathbf{g(r)}=\partial U/\partial r=(GM/r^2)\mathbf{e_r} \qquad (3.7)$$

In gravity exploration, only the vertical components of the acceleration is measured so that we are normally concerned with $\mathbf{g_z}$, hence forth, it is written simply as g in applying the gravity at the surface of potential features.

3.2.5 Three Dimensional Potential

If the mass distribution is three dimensional, the potential of an element mass dm at a distance **r** from the centre of mass is

$$dU = GdM/r=G\rho dx\, dy\, dz/r \qquad (3.8)$$

Where,

ρ the density

$\mathbf{r}$ = $(x^2+y^2+z^2)^{1/2}$

So that, the potential of the total mass M is found as:

$$\mathbf{U(x,y,z)=G\int\int\int 1/r\ \rho dx\, dy\, dz} \qquad (3.9)$$

In cylindrical coordinates, dV= r dr dϕ dz, the u (r, ϕ , z) is :

$$\mathbf{U(r,\ \phi\ ,z)=G\int\int\int}\rho\ dr\ d\phi\ dz \qquad (3.10)$$

In spherical coordinates, $dV= r^2 \sin\theta \, dr \, d\theta \, d\phi$, we get, $U(r, \theta,\phi)$,

$$\mathbf{U(r, \theta,\phi)=G\int\int\int \rho \, r \sin\theta \, dr \, d\theta \, d\phi} \qquad (3.11)$$

The acceleration of gravity in the direction of z- axis, what we have actually measured, is referred to us simply g is calculated from:

$$g_z = \partial u/\partial z$$

Thus, we have

$$\mathbf{g_z = -G\int\int\int z/r^3 \, \rho dx \, dy \, dz}$$

(3.12)

Cylindrical,

$$\mathbf{g_{z=} \; -G\int\int\int \rho z/r^2 \sin\theta \, dr \; d\phi \, dz} \qquad (3.13)$$

Spherical,

$$\mathbf{g_z = -G\int\int\int \rho \, z/r \sin\theta \, dr \, d\theta \, d\phi}$$

$$\mathbf{= -G\int\int\int \rho \sin\theta \cos\theta \, dr \, d\theta \, d\phi} \qquad (3.14)$$

3.2.6. Two Dimensional Potential

If the mass distribution is two dimensional, which occur when the mass is very long in the Y direction, and has uniform cross-section of arbitrary shape in the XZ-plane.
The logarithmic potential is given by

$$\mathbf{U(x,z)= \quad 2G\int\int \rho_{log}(1/r) \quad dx\ dy} \qquad (3.15)$$

Then, the gravity effect for the two dimensional body will be:

$$\mathbf{g_z} = \quad \partial u/\partial z \quad \mathbf{=-G\int\int \rho z/r^2 \ dx \ dz} \qquad (3.16)$$

Where $\mathbf{r}= (x^2 + z^2)^{1/2}$

Note that, if the ρ is a function of the coordinates as well, the potential can be calculated only for a few simple shapes. These are the basic equations for calculating the gravity effects of bodies of uniform density. The use of equations 3.12 to 3.16 make it possible to obtain closed analytical expressions for the gravity effects of bodies of regular shape such as sphere, cylinder, horizontal slab etc. Of these the most widely used is the gravity formula for an infinitely extended horizontal slab that has been employed in computation of Bouguer slab, given by,

$$\mathbf{g_B=2\pi G\rho Z} \qquad (3.17)$$

Where**ρ,** is the density, and **Z**, is the thickness of the slab.

In gravity work, computations are often simplified using the scalar potential, U, instead of the vector g. The first derivative of U in any direction gives the components of gravity in that direction, as a result of a potential field approach provides computational flexibility. Equipotential surface are regions where U is constant. The geoid is the most easily recognized equipotential surface, which is assumed to be horizontal and orthogonal to the direction of gravity.

3.3 Gravity of a Rotating Sphere

Consider a small mass m moving with velocity v on the surface of rotating spherical earth of angular velocity ω .Forces per unit mass acted on m can be verified as flows:

g_m the attractive force per unit mass acting on a mass m due to the earth's mass M_E is given by equation (3.3)

$$g_m = G(M_E / \mathbf{R_E}^2) \mathbf{e}_r \quad , \qquad (3.18)$$

Where, $\mathbf{e}_r$ is a unit vector directed towards the earth's center along its radius $\mathbf{R_E}$

$\mathbf{g_\omega}$ the centrifugal force per unit mass acting on m due to earth's rotation with ω. Thus,

$$\mathbf{g_\omega = \omega (\omega x R_E)} \qquad (3.19)$$

C the coriolis force per unit mass acting on m due to its motion, with V. The equation is in a form:

$$\mathbf{C=2(\omega \times V)} \qquad (3.20)$$

C has a zero value if m is at rest on the earth's surface.

T the tidal force per unit mass acting on m due to mass attraction of other heavenly bodies. This is rarely easy to express with a simplified mathematical formula due to the variation in position and number of heavenly bodies that have an impact on m. However, of particular tidal effects of the sun and moon are occasionally considered, and have taken care of this study.

The resultant force per unit mass acting on a mass m in accord with these physical quantities verified above is termed as gravity, g, that is,

$$g=g_m + \mathbf{g_\omega} + \mathbf{C} + \mathbf{T} \qquad (3.21)$$

The effects of the coriolis **C** and tidal **T** are usually considered negligible in actual work. Hence forth, the gravity g refers to the superimposed effects of both earth's mass attraction g_m and rotation $\mathbf{g_\omega}$ .Thus; the expression of equation 3.21) reduces to:

$$g=g_m + \mathbf{g_\omega} \qquad (3.22)$$

And the components,

$$g_m = g_{mr}\,\mathbf{e_r}\text{ ,and }\mathbf{g_\omega} = g_{\omega r}\,(\,-\mathbf{e_r}\,) + g_{\omega t}\,(\mathbf{e}\,)$$

Where, er a unit vector radially inward; g_m, $g_{\omega r}$, magnitudes along $\mathbf{e_r}$; $g_{\omega t}$, magnitudes along **e** .

Evidently, the tangential component has not have an effect on m and therefore equation (3.22) is modified to:

$$g= (g_{mr} - g_{\omega r}) \mathbf{e_r} \qquad (3.23)$$

Finally, plug corresponding values to find:

$$g = [\, G M_E / \mathbf{R_E}^2 - \omega^2 R_E \cos^2(\varphi) \,] \; \mathbf{e}_r \qquad (3.24)$$

This expression is the basic equation of gravitational acceleration or intensity of gravitational acceleration.

The value of gravity at the equator $g_{e,}\varphi=0$, equation (3.24) becomes:

$$g_e = [G M_E / \mathbf{R_E}^2 - \omega^2 R_E \,] \; \mathbf{e}_r \qquad (3.25)$$

, and at the poles $g_{p, \pm} 90^0$ we find

$$g_p = [G M_E / \mathbf{R_E}^2 \,] \; \mathbf{e}_r \qquad (3.26)$$

Thus, the gravity difference Δg_t is:

$$\Delta g_t = g_p - g_e = (\omega^2 R_E) \; \mathbf{e}_r \qquad (3.27)$$

$\Delta g_t = g_p - g_e$ =3.4 gal

However, for the real earth, observed values of (pendulum observations) g are found to be 983.218 and 978.032 gals, at the poles and equator, respectively. These values give rise to find the actual gravity difference as

$\Delta g_{ob} = g_p - g_e = 5.2$ gal (3.28)

Hence, the discrepancy between the observed $\Delta g_{ob,}$ for the real earth and theoretically computed $\Delta g_{t,}$ for a spherically symmetric earth model gives earthly sights of: The shape of the earth is not spherical; the shape of the earth is rotationally distorted one such that it is flattened at the poles and bulged at equator; gravity varies as a function of latitude Φ.

3.3.2 Gravity on a Rotating Ellipsoid

Rotating Ellipsoid

In modeling the earth as a rotating sphere of uniform density, it is discovered the shape of the earth is a rotationally distorted one that is flattened at the poles and bulged at the equator. Virtuously, the balance of gravitational and centrifugal effects shape the earth in to more or less an ellipsoid, which is (a flattened sphere) an ellipsoid of revolution, i.e., a surface generated by the rotation of an ellipse about its minor axis with the major axis generating the equatorial plane. The angular velocity ω, the density distribution ρ, equatorial radius Re, and shorter polar radius $R_{p,}$ as well as the ellipticity e, are used to describe the shape of the ellipsoid. Ellipticity e is defined by:

$$e = (R_e - R_p)/R_e \quad (3.29)$$

To describe the gravity of the earth that account for flattening and centrifugal effect, both of which change with latitude a theoretical surface of the earth is defined by an equipotential surface and this is considered to be an ellipsoid revolution with ellipticity e, such that it is related to the mean sea-level surface with excess land masses removed

and ocean deeps filled. The force of gravity, is by definition every where perpendicular to the surface.

Progressively more, the earth's gravity potential W (X, Y, Z) can be defined by the means of formula follows.

$$W(X, Y, Z) = \nu_{\varphi} + U_m \quad (3.30)$$

Where ν_{φ}, centrifugal potential; Um, mass gravitational potential.

As a result,

$$W(X, Y, Z) = G\iiint \rho d\nu / r + 1/2\omega^2 (X^2 + Y^2) \quad (3.31)$$

The gravity potential at the surface of the reference ellipsoid, which is an equipotential surface, is consequently be specified by,

$$W(X,Y,Z) = Wo = \text{constant} \quad (3.32)$$

The gradient of the gravity potential on a rotating reference ellipsoid at latitude ϕ is the normal gravity vector $g(\phi)$ and this pointed out,

$$g(\phi) = \text{grade } W \quad (3.33)$$

Applying further mathematical computations and approximations, the theoretical gravity (the normal gravity) value g (ϕ) at any latitude ϕ on rotating reference ellipsoid is derived in a form given here below.

$$g(\phi) = = g_o [1 + C_1 \sin^2(\phi) + C_2 \sin^4(\phi)] \quad (3.34)$$

Or, consistently

$$g(\phi) = g_o [1 + B_1 \sin^2(\phi) - B_2 \sin^2(2\phi)] \quad (3.35)$$

The constants C1,C2 and B1, B2 depend on ellipticity e and the rate of rotation ω.The value of these constants are found from careful studies of astronomical measurements and observation of orbiting satellites .In addition $g_o = g_e$ is the value of the normal gravity on the equator , ϕ =0 and

its value is determined through detail observations and analytical studies.

The Geoid

The theoretical gravity expression (3-34) is a very crude approximation. Theoretical assumptions underlying this approach is that there are no undulations in the earth's surface unlike wise to the actual earth surface, that encompass continental elevations, highly elevated land and ocean depressions, all referred to sea level.

For practical work a physical surface on the earth referred to a practical mean sea level (equipotential) surface is defined for making gravity measurements (and therefore be related to the reference ellipsoid theoretical earth model) .It is known as the geoid and is defined as average sea level over oceans and over the surface of sea water which would lies in canals, as if it cut through the land masses.

Markedly, the value of gravity that would have occurred as if it were measured on the geoid surface, and theoretically computed on the reference ellipsoid surface do not- in fact, never could coincide at all point since the geoid is wrapped upward under the continental masses due to attracting material above and downward over the ocean basins, henceforward, a deviation existed in between of the equipotential surfaces, this is resulted from a gravitational attraction of an invisible anomalous mass at a point of concern .The deviation between the measured gravity potential W(X,Y, Z) and the theoretical gravity potential U(X, Y, Z) is denoted by T(X,Y,Z) .i.e.

$$W(X, Y, Z) = U(X,Y,Z) + T(X,Y, Z) \qquad (3.36)$$

T(X,Y,Z) Is called anomalous potential, or disturbing potential (Heiskanen and Moriz, 1967). T is abandoned for small regions. Thus the potential on the geoid referred to the average sea level surface W(X,Y, Z) = Wo, is

compared with the potential on the reference ellipsoid referred to the same average sea level surface u(X,Y,Z)=Uo ,on underlying assumption that they are potential of identical equipotential surface, Clearly,

Uo =Wo (3.37)

Taken care of the gravity vector g at a point of the geoid and the theoretical gravity g(ϕ) a point of the reference ellipsoid, the gravity anomaly vector is defined by the magnitude difference in between.

$\Delta g=g-g(\Phi)$ (3.38)

The difference in direction is the deflection of the vertical angle (θ). Hence g is the gravity value observed (g_{obs}) at a point on the actual surface of the earth and reduced to the geoid point; g (φ) is the theoretical value of the ellipsoid point.

Gravity anomalies are determined as a result of density irregularity of the earth, mainly of the crust. Therefore gravity anomalies are imprinted up on which valuable geological in formations are obtained for exploration.

3.3.3 Normal (Theoretical) Gravity

We have found a general formula g (φ) for calculating gravity on the ideal model of the earth. This model is known as either the reference ellipsoid or the normal ellipsoid, which is most closely related to the mean sea-level surface of the earth.

The reference ellipsoid can be described by its equatorial radius R_e, ellipticity e, and angular velocity ω. These values are obtained from astronomical observations and orbits of artificial satellites and are

combined to find the constants C_1,C_2 and B_1,B_2 of the theoretical gravity Equations (3.34) and(3.35).

Furthermore, we should heed attention in order to find the value of the gravity go = ge on the equator of the reference ellipsoid.

In 1930, an institution known as the International Union of Geology and Geophysics (IUGG) chose the most appropriate reference ellipsoid and the following values were adopted by it:

R_e= 6, 378.388 meters
e= 1/297
ω= 7.2921151x10^-5 radian /second
g_e = 978.049 Gals
And the values of B_1,B_2 shown below have been derived
B1 = 0.0052884
B2 = 0.0000059

These values were combined with Equation 3.35 to adopt the 1930 International Gravity Formula.

$$g(\phi)_{1930} = 978.049\ [1+0.0052884\sin^2(\phi) - 0.0000059\sin^2(2\phi)]\ \text{gal} \quad (3.39)$$

Studious researches conducted on the heel of the 1930 gravity formula had emerged with more precise values that were later in 1967 further refined and forwarded new values of reference ellipsoid indicated below:

R_p = 6.378,160 meters
R_e = 6.356774.5

e = 1/298.247

ω = 7.2921151467x10^{-5} radian/second

g_e=. 978.031846 gals

And the determined values of C1 and C2 were

C1 = 0.005278895

C2 = 0.000023462

The Normal gravity formula modified by combining these values in Equation 3.31 is:

$g(\phi)_{1967}$ = 978.031846 [1+0.005278895 $\sin^2(\phi)$ + 0.000023462$\sin^4(\phi)$] gal (3.40)

This is called the 1967 geodetic reference system formula (GRS 67 formula).

Further more, IUGG modified the reference ellipsoid in 1980 though the modifications have little importance on exploration geophysics. Nevertheless the GRS67 formula is quite accurate enough for gravity survey result analysis.

Meanwhile, the theoretical formula can be compiled as follows:

1930 Formula

$g(\varphi)_{1930}$ = { 978049 [1 + 0.0052884 $\sin^2(\varphi)$ - 0.0000059 $\sin^2(2\varphi)$] } mgal

(3.41)

(" potential theory in gravity and magnetic application " by Richard Blakey,1995,Cambridge University Press,p135.)

1967 Formula

$$g(\varphi)_{1967} = \{ 978031.846 [1+0.005278895 \sin^2(\varphi) + 0.00002346 \sin^4(\varphi)] \} \text{ mgal} \quad (3.42)$$

(Sheriff, Encyclopedic Dictionary of Exploration Geophysics 2nd Edition, 1984 p141)

1984 formula:

$$g(\varphi) = \{ 978032.67714 [1 + 00193185138639 \sin^2(\varphi) / \text{sqrt}(1-0.00669437999013 \sin^2(\varphi)] \} \text{ mgal} \quad (3.43)$$

(" potential theory in gravity and magnetic application " by Richard Blakey,1995,Cambridge University Press,p136.)

Where $g(\varphi)$, theoretical value of gravity in milligals (latitude correction) ; φ , is latitude of the station φ

3.4 World Wide Network of Gravity Base Station

Accurate values of absolute gravity and the worldwide distribution (primary base station) can be obtained from IGSN-71.

The gravity difference between one of these base stations and every of the gravity stations may be found in particular gravity survey hence we can

easily calculate gravity, g at the survey station referred to the IGSN-71 gravity datum. This can be explained here below:

$$g = g_r + \Delta g \tag{3.44}$$

Where g, the absolute gravity value at a station; g_r the reference absolute gravity value at the base station; Δg, the gravity difference between the base station and a station or other base station required for particular gravity survey that would be tied and drift corrected, i.e.,

$$\Delta g = \Delta g_h - \delta g \tag{3.45}$$

Where Δg_h, scale and instrument height corrected difference milligal value; δg, the combined tied and drift correction between these reading times in milligals.

In this way we can obtain accurate values of gravity at a worldwide distribution of gravity stations and therefore these gravity stations make up what is called IGSN-71.

3.5 Components of Gravity Reduction

Measured gravity values at gravity stations' covering an area of interest on earth's surface varies as a result of variation in latitude, elevation, topography of the surrounding terrain, earth –tides and density variation in the sub-surface. Of particular interest in exploration is changes in gravity values caused by density irregularities associated with geological features. However, in order to account for effects associated with non-geological features of interest, measured gravity values should be reduced to an equipotential datum such as to the geoid surface

whereby, these reduced values can be directly compared with their respective theoretical gravity values in a mathematical equipotential datum as to the reference ellipsoid.

Thus, terse gravity reductions must be made to the measured gravity values to reduce the gravity station to the geoid surface for the computation of gravity anomalies.

Accordingly, the standard components of gravity reductions can be categorized as follows:

3.5.1 Drift Correction

The gravity readings of all gravimeters change non –zero values with time, even when set over a station. Thus, drift is a continual change of the gravity readings with time caused mainly by elastic creep in the gravimeter springs; besides, ambient environment variation of temperature and /or pressure, even the gravimeter is self –compensated. Under normal operating condition, the drift in gravity reading at a station may be from a few hundredths (of a mgal) to about tenths of a mgal per hour, but drift rates greater than tenths of a mgl per hour have been observed under extreme ambient environment changes.

In order to correct for drift, the usual method is to reoccupy one or more stations periodically during a gravity survey. The maximum time allowable depends on the accuracy required in the survey that would seldom be greater than two or three hours. So, the difference obtained are arranged against the time between two readings at a station A “drift” curve can then be drawn and the correction read off it .In a relative high accurate survey it is advisable to determine the drift curve by a least

squares method. This is usually straightforward most gravimeters drift linearly with time, parabolic or other drift functions are however, uncommon.

The intermediate gravity stations, which are occupied only once, can then be corrected for the drift, which has occurred during the appropriate fraction of time interval between reoccupations. These corrections can be taken directly of the drift curve such that positive drift requires negative correction and vice –versa.

Since there is no way of allowing for possible erratic drift between control stations, we can only draw straight lines joining these points on the drift curve and trust that the variation was linear with time (R.S.Sheriff, 1978 et al).None linear changes may be caused by earth tides, by repeating station within two-three hours or less it is possible to remove tidal variation reasonably well.

3.5.2. Tide Correction

Gravimeters are quite sensitive enough to record the cyclic change in gravity caused by the combined mass attraction of the sun and the moon as their position change with respect time. These tidal changes have amplitudes as large as 0.3mgal (Sheriff,R.E. and et-al,1978). In addition the maximum rate of tidal variations is about 0.05 mgal (Sharma, V., 1997).

Purely, the tidal –variation of gravity can be derived from knowledge of positions of the sun and the moon as a function of time. However, because of the variations is smooth and relatively too low it is often included in the drift correction. Nevertheless, in high accurate gravity

work this fluctuation of gravity δg_{ct} can be calculated using an equation based on the masses of the moon and the sun, and their position relative to a station.

$$\delta g_{ct} = 3/2\sigma G R_E \left[M_m/r_m^3 \left(\cos 2\vartheta_m + 1/3 \right) + M_s/r_s^3 \left(\cos 2\vartheta_s + 1/3 \right) \right] \quad (3.46)$$

where R_E is the earths radius, M_m and M_s are the lunar and solar masses, and their distances from the earth's center are r_m and r_s. The value δ**=1.16** accounts for the way that the earth itself is stretched elastically by the tidal force. Angles ϑ_m and ϑ_s between line from the earth's center to the station and lines from the earth center to the moon and sun change time. These angles can be calculated for any particular time from formulas based on astronomical measurements of the relative motions of the earth, moon, and sun. Because these formulas are long and complicated, a computer program is ordinarily used to make the calculation. Alternatively, appropriate corrections can be made by referring to special tables (example, tables regularly published in advance for each year in geophysical prospecting, the journal of the European Association of exploration geophysicists).

Drift –tidal correction

During gravity survey certain stations should be reoccupied at a very least every two –three hours to determine both drift and tide corrections properly. The reoccupations are used to prepare a curve (graph) from which the change in gravity with time is flaunted because of cyclic tidal changes and non cyclic gravimeter drift. For some surveys reoccupations more than once or twice a day are impractical .If such is a case it is necessary to combine these few repeated readings with tidal fluctuations

computed from equation (3.46) to prepare curve of time variations. After a curve (showing cyclic and non cyclic variations) is prepared for the durations of a gravity survey, corrections can then be found by interpolation at the times when reading were made at all the stations .Effectively , methods of least squares are encouraged .

3.5.3 Free –Air Reduction

Free – air reduction accounts for the variation of change in gravity with elevation above the plane of reduction, the geoid .The gravity **g** varies in inverse proportion to the square of the distance from the earth's center, hence it should be necessary to correct for the changes in elevation between stations so that all measured relative gravity values are reduced to the geoid surface. This is known as free-air reduction since it takes no account for the masses contained between the station and the geoid surface .It can be obtained by differentiating the scalar inverse square law equation (3.3) with respect to the earth's radius R_E.Thus , the free air gradient of gravity **g** gives a correction for the station elevation :

$$\delta g_F(h) = \left(\partial g / \partial h\right)h \cong \left[\partial g(\Phi)/\partial h\right] h$$

As a result,

$$\delta g_F(h) = 0.30859h \text{ mgal} \qquad (3.47)$$

Where $\delta g_F(h)$, Free-air correction in milligals;**h** station elevation above the geoid in meters.

The free –air correction $\delta g_F(h)$ given by equation (3.47) is sufficiently accurate for most purposes.

Alternatively, free -air correction may be computed using the formula follows.

$$\delta g_F(h,\Phi) = [\,0.308767763 - 0.000439834\sin^2(\Phi) - 0.000000072124602h\,]h \quad (3.48)$$

(Heiskanen and moritZ, 1967, physical geodesy: Sanfransisco, Free man Press)

This formula (3.48) accounts for non linearity of free-air reduction as a function of both latitude**Φ,** and height above the geoid **h**.

The free –air correction should be added to a measured relative gravity value if the station lies above the geoid surface and subtracted if it lies below it .

Elevation difference from the geoid surface should be measured to an accuracy of better than 4 cm in order that the survey may be accurate to with in 0.01mgal.

3.5.4. Bouguer Reduction

The Bouguer reduction accounts for the gravitational attraction of mass that exists between the station elevation and the geoid surface, which was not taken care of the free- air reduction.

If the station were centrally located on a plateau of infinite horizontal extent with uniform thickness **h** above the geoid surface and density ρ the measured relative gravity value would be increased by the effect of

this slab that exists between the station elevation **h** and the geoid surface. The Bouguer correction derived by modeling the slab (now referred to as the Bouguer slab) of infinite horizontal extent is resulted in the form;

$$\delta g_B (\rho,h) = 2\pi G\rho h \qquad (3.49)$$

Consequently,

$$\delta g_B (\rho,h) = 0.04198088\rho h \ \text{mgal} \qquad (3.50)$$

The Bouguer reduction includes a correction for water depth and ice thickness if there exists. Accordingly, the Bouguer correction for the mass of rock that exists between the station elevation and the geoid; besides, for water depth and ice thickness required can be calculated from the following formula:

$$\mathbf{\delta g_B(\rho,h) = 0.04198088 [\rho h + (\rho_w - \rho) h_w + (\rho_i - \rho_w) h_i]} \qquad (3.51)$$

The Bouguer correction must be subtracted from the measured relative gravity value if the station lies above the geoid surface and vice versa.

When gravity measurements are made below the earth's surface the slab of mass between stations exerts an attraction on a unit mass placed at lower as well as higher station level. As consequence, it is down ward on higher station and upward on the lower one. These attractions being in

opposite directions, the gravity difference in between caused by the slab is doubled. i.e., the Bouguer correction is:

$$\delta g_B(\rho,d) = 4\pi G\rho d = 0.08396176\rho d \quad \text{mgal} \qquad (3.52)$$

Where**ρ**, Bouguer slab density in g/cm^3; d, the thickness of the slab in meters.

Two assumptions are considered in driving the Bouger reduction; the Bouguer slab is of uniform density and infinite horizontal extent. Actually, neither is valid. In order to accommodate the first, one would need to have considerable knowledge of the local geology as to rock type and actual densities. The second is taken care of the next reduction.

3.5.5 Terrain Correction

In driving the Bouguer reduction it was assumed that the actual surface of the earth (in the vicinity of the station) by a subdue topography i.e the terrain around a station is perfectly plain which doesn't happen in reality. In reality there exists hills or mountains rising above the level of the gravity station depression and valleys (lack of material) below it. Hence, terrain correction is applied to account for a topographic irregularity around the gravity station when gravity survey is carried out in an area of rugged terrain.

Terrain correction accounts for topographic undulations around the gravity station, that is, land masses rising above the gravity stations and lack of material below. It is obvious that both of these topographic undulations affect the gravity measurements in the same sense, reducing the gravity because of upward attractions (such as hills) or lack of

downward attraction (such as valleys). And therefore the terrain correction is always added to the station measured gravity value.

Terrain irregularity (hill, knoll, slope, etc.) will exert an attraction directly proportional to its density. The vertical component δg_t of this attraction will be directly upwards and reduce the gravity at a station. A value of this magnitude must therefore be added to the measured gravity value at a station. A valley in proximity of a gravity station is a negative mass and the vertical component of its attraction will also be directed upwards giving rise to an additive terrain correction.

There may be several methods for computing the terrain correction all of which require detailed knowledge of the terrain in the proximity of a gravity station; beside, a good topographic map commonly with contour interval approximately 10 meters or smaller extended considerably beyond the survey area and/or clinometers measurements. The usual method is to estimate the terrain correction with combined effects of compartments bounded by concentric rings in proximity of a gravity station.

The correction in such a compartment is:

$$\delta g_t\ (r, \theta) = G\rho\theta \{(r_O - r_i) + (r_i^2 + \Delta Z^2)^{1/2} - (r_o^2 + \Delta Z^2)^{1/2}\} \qquad (3.53)$$

Where r_i, r_O are the radii of the inner and outer rings bounded the compartment; θ is the compartment angle (radians), and

$\Delta Z = / Z_S - Z_a /$

Where Zs, Station elevation; Za , Average elevation in the compartment.

The terrain correction Δg_T is the sum of the contribution of all compartments:

$\delta g_{T = n\,n}\, \delta g_t\ (r, \theta)$

(3.54)

3. 5 .6. Curvature (Bullard B) Correction

The purpose of the curvature correction as a step in produced the Bouguer gravity anomaly is to convert the geometry for the Bouguer reduction from an infinite slab to a spherical cap whose thickness is the elevation of the station and radius (arc length) from the station is 166.735 kM .Curvature correction (example 1.1 mgal at 1000m, 1.5 mgal at 3000m, 0.2 mgal at 4000m,-1.5mgal at 5000m and -3 mgal at 6000m),and latitude (in dozens microgal). Lafehr's formula can be used for curvature correction. (T.R. Lafehr, 1991, An exact solution for the gravity curvature (Bullard B) correction: Geophysics, V56, PP79-1184).

In this particular research, the author takes no account for curvature correction, on the basis of a reason that the curvature would have scarcely merits (a significant impact) in a small area accompanied with relatively low station elevations.

3.6. Gravity Anomaly

The earth gravity field compromises various imprints of geological features associated with several physical entities. Of distinct concern in gravity prospecting is imprints related to density contrasts of sub - surface earth materials. These can be recognized by comparing measured gravity values reduced to geoid surface (practical equipotential surface) in accord with the standard components of reduction described in

section 3.5 with the corresponding theoretical gravity values computed on the reference ellipsoid (theoretical equipotential) following the scheme outline in section 3.3.3.Obviously, the reduced measured gravity values at the datum level geoid can be compared with the theoretical gravity values at the datum level reference ellipsoid in respect to their positions, that is, the theoretical gravity value **g(Φ)**can be subtracted from the properly adjusted measured gravity value **g** to obtain a value called gravity anomaly .The word anomaly implies the deviation from the regular. Of particular concern here is the deviation in gravity value related to the geologic features resulted the actual earth in contrast with the reference ellipsoid. These gravity anomalies are values of interest that exploration geophysicist interprets to find out valuable in formation about the geologic features as well as structures of the earth imprinted on the gravity.

If g is the measured gravity value at station elevation h above the geoid, it should be reduced to sea level (geoid) to compare with g (Φ), the theoretical value on reference ellipsoid of the same latitude Φ. Therefore the gravity anomaly at a station is defined by,

$$\Delta \mathbf{g} = \mathbf{g_G} - \mathbf{g}(\Phi) \qquad (3.55)$$

Where Δg, the gravity anomaly; g_G, measured gravity value of a station reduced to geoid surface; g (Φ), theoretical gravity of the station latitude Φ.

Depend on components of reduction applied for a gravity station, the gravity anomalies can be categorized in a steady's purpose.

3.6.1. The Free –Air Gravity Anomaly

If only the free-air reduction, $\delta g_F(h)$ / $\delta g_F(h,\Phi)$ has been applied, the free air gravity anomaly $\Delta g_F(g,h,\Phi)$ is defined as:

$$\Delta g_F(g,h,\Phi) = g + \delta g_F(h) - g(\Phi) \qquad (3.56)$$

Alternatively,

$$\Delta g_F(g,h,\Phi) = g + \delta g_F(h,\Phi) - g(\Phi) \qquad (3.57)$$

Where $\Delta g_F(g,h,\Phi)$, Free – air gravity anomaly in milligrams; **g,** Tide and drift corrected observed gravity; $\delta g_F(h)$ / $\delta g_F(h,\Phi)$, Free-air gradient correction from (3.47)/(3.48) ; $g(\Phi)$, Theoretical gravity calculated for a station latitude Φ using GRS-67 gravity formula (3.42) or optional Formulas are available in section (3.3.3).

In this study, Equation (3.57) has been applied throughout the computation of the Free – air gravity values. The aforementioned Formula could be displayed in a more explanatory form:

$$\Delta g_F(g,h,\Phi) = g + [0.308767763 - 0.000439834 \sin^2(\Phi) - 0.000000072124602h]h - g(\Phi)_{1967} \qquad (3.58)$$

(Heiskanen and moritZ, 1967, physical geodesy: Sanfransisco, Free man Press)

This formula accounts for non-linearity of the free-air gravity as a function of latitude and height above the geoid datum.

Free –air gravity anomaly generally forms the basis for the interpretation of gravity data in marine environment. Moreover it provides abroad assessment of the degree of isostatic computation of an area. Values from land gravity surveys show strong correlation with local topography since gravity effects of rock masses are not taken care of the free-air reduction. Hence it is not well suited for local gravity on land to reveal considerably valuable information about the actual geologic imprints desired in prospecting.

3.6.2. The Simple Bouguer Gravity Anomaly

The simple Bouguer gravity anomaly corrects the free-air gravity anomaly for the material slab exists between the station elevation and the geoid surface however terrain effect is not taken care of here. In consent with the Bouguer reduction correction $\delta g_B (\rho, h)$ [(3.50)] described in section 3.5.4, the simple Bouguer gravity anomaly, $\Delta g_{SB} (g, h, \Phi, \rho)$ is determined by:

$$\Delta g_{SB} (g,h,\Phi , \rho) = \Delta g_F(g, h, \Phi) - \delta g_B (\rho,h) - g_c \qquad (3.59)$$

$$\Delta g_{SB} (g,h,\Phi , \rho) = g + \delta g_F (h,\Phi) - \delta g_B (\rho,h) - g_c - g (\Phi) \qquad (3.60)$$

Where $\Delta g_F(g, h, \Phi)$, Free-air gravity anomaly; g_c, Curvature (Bullard B) correction outlined in section 3.5.6 in addition; ρ, average subsurface

density; **h,** station elevation with reference to geoidal surface (h=o); **g (Φ),** Theoretical gravity calculated from formulas described in section (3.3.3).

In case of this study, the curvature correction $\mathbf{g_c}$ has not been considered and therefore, the formula (3.60) has been reduced to a form as;

$$\Delta g_{SB}\,(\,g,\,h,\Phi\,,\,\rho\,) = g + \delta g_F\,(\,h,\Phi\,) - 0.04198088\rho h - g(\Phi)_{1967} \qquad (3.61)$$

3.6.3. Complete Bouguer Gravity Anomaly

The complete Bouguer gravity anomaly corrects the simple Bouguer gravity anomaly for topographic irregularities of the earth in the vicinity of a gravity station.

In consent with the terrain correction explained in section 3.5.5, the terrain corrected Bouguer gravity anomaly is found with ease. To mention, this anomaly takes account of the Free-air, Bouguer slab, and terrain reductions.

Truly, if the earth crust had no lateral variation in density, a set of measured gravity values taken care of the aforementioned reductions would be identical. Of this juncture, differences in the properly corrected values constitute a gravity anomaly, known as the complete or terrain corrected Bouguer gravity anomaly, the result of lateral variations in sub- surface densities.

Whenever all of the preceding reductions have been applied to the measured gravity value, the terrain corrected Bouguur gravity anomaly for the station is obtained by:

$$\Delta g_{C\text{-}B}\,(\,g,h,\Phi\,,\,\rho\,) \;=\; \Delta g_{SB}\,(\,g,\,h,\Phi\,,\,\rho\,) \;+\; \delta g_T \qquad (3.62)$$

Where $\Delta g_{C\text{-}B}\,(\,g,h,\Phi\,,\,\rho\,)$, Complete Bouguer gravity anomaly; $\Delta g_{SB}\,(\,g,\,h,\Phi\,,\,\rho\,)$, Simple Bourguer gravity anomaly from (3.60) ; δg_T, supplied terrain correction.

Formula (3.62) can be equally expressed by

$$\Delta g_{C\text{-}B}\,(\,g,h,\Phi\,,\,\rho\,) \;=\; g + \delta g_F\,(\,h,\Phi\,) - \delta g_B\,(\,\rho,h\,) + \delta g_T - g_c \;-\; g\,(\Phi) \qquad (3.63)$$

Formula (3.61) in conjunction with (3.62/63) is adopted in this study.

3.7 Separation of Anomalies and/or Wave Length Filtering

The measured value of gravity and therefore also the reduced Bouguer gravity anomaly represent the superimposed effects of many geologic features at various depths. Any pattern of variation observed on the compiled Bouguer gravity anomaly is a combination of local sources (or residual sources, referred to source of interest) and broader or more distant regional sources. Nowhere can be measured a gravity anomaly from a one source that is not distorted by overlapping anomalies from other sources.

Certainly, in some locations gravity anomalies indicating structural features of particular concern are dominant that the distortion by other anomalies is minor. In other locations, however are almost completely obscured. As consequence attempts are made to separate (isolate) individual anomalies from the patterns of variations depicted on the compiled gravity a normally.

Nevertheless more concern have been given to the problem of separating the local residual and regional anomalies, there is rarely come to accomplish complete separation. Nonetheless, several methods have been developed for isolating the principal features of different gravity anomalies.

The methods are quite useful to discern obscure and halted gravity anomalies in clearer focus.

Methods adopted for this particular study are verified here below.

3.7.1. Gridding or Digitizing Data

Most residualzing and filtering schemes can be applied with ease whenever the Bouguer gravity anomaly values are found at regularly spaced intervals. Practical useful is to determine value at a square grid points before attempted to separate and /or filter anomalies. This can be performed well by drawing or overlaying on a gravity anomaly contour map an appropriate grid of points or intersecting lines. The value at a point or line intersection is then found by interpolation or using computer programs (like surfer). The spacing should be reasonably taken so that the contour patterns could be reproduced from the grid values.

The gravity anomaly values and the positions of the irregularly spaced stations are required to carry out the interpolation based on the stations in proximity of a grid point. The process of finding regularly spaced values is called griddling or digitizing the compiled gravity anomaly.

3.7.2. Second Vertical Derivative Methods

A second vertical derivative enhances short wave length anomalies relative to long wave length anomalies. Thus, second vertical derivative amounts to horizontal curvature of field and tends to delineate the edges of anomalous body. In fact, second derivatives are a measure of curvature, and large curvatures are associated with shallow or residual anomalies. Further more, it is possible to obtain $(\partial^2 \Delta g / \partial Z^2)$ from the horizontal second derivatives, since the gravity field satisfies Lap lace's equation (Elkins, 1951).

More accurate determinations of the second vertical derivative $(\partial^2 \Delta g / \partial Z^2)$ can be obtained by methods, which are entirely analytical using several concentric circles (generally 3) of different radii. The effect of each circle is weighted by a coefficient term. This technique has been developed independently by several people (Henderson and Zietz, 1949, Elkins, 1951, Dean, 1958). Their results are all of the form:

$$(\partial^2 \Delta g / \partial Z^2) = K/S^2 (W_0 \Delta g_0 + W_1 \Delta g_1 + W_2 \Delta g_2 + \ldots) \quad (3.64)$$

Where Δg_0, the Bouguer gravity at the station where the second derivative is being determined (at the center of the circles) ;Δg_1 , Δg_2 , . . .

are average values on successive circles;W_0 , W_1 , . . .are weighing coefficients such that $\sum W_I = 0$; K , numerical factor; S, the grid spacing.

The circle radii are normally selected on the basis of the grid dimensions. For example, if the survey is on a square grid with spacing S the successive radii generally are S, √2S, √5S, etc, with $r_0 = 0$ for the first term which represents the common center. One form of equation (3.64), which works very well (Henderson and Zietz, 1949) is

$$(\partial^2 \Delta g / \partial Z^2) = 2 (3 \Delta g_0 - 4 \Delta g_1 + \Delta g_2) \qquad (3.65)$$

Obviously, there may be some bias in using (3.64), which depends on the coefficients employed.
Gurta and Ramani (1982) show an application to mineral exploration.

3.7.3. Empirical Gridding Methods

These methods originally described by Griffin (1947) are really simple way of separating regional anomaly by average estimation. The regional anomaly value at a station is estimated as the average of values from the surrounding area, that is, the regional is considered to be the average value of Bouger gravity in the vicinity of the station, and is determined by averaging actual values on the circumference of a circle centered at the station

3.7.4. Wave Length Filtering

Wavelength filtering is a mathematical operation that can be used to enhance the appearance of either regional anomaly patterns or local anomaly patterns. The foregoing methods attempt to separate regional

and local anomalies based on the degree of smoothness of anomalies we are moving, or filtering out, effects represented by certain wavelength. Hence, the name wave length filtering can also be done by transforming data to a wave number – wave number domain using a two-dimensional Fourier transform, removing certain wavelength components, and then using an inverse transformation to reconstitute the map, but with certain wavelength removed.

Therefore, these kinds of wavelength filtering have helped to bring a clearer focus, the approximate sizes and shapes of other wise obscure local anomalies. In similar way, we can reproduce only the regional anomalies and filtering out local anomalies by removing short wave lengths. Again, this result is not perfect because some of the remaining long wavelength anomalies may be related to local anomalies. Nevertheless, a clear view of regional patterns of variations is produced.

The type of filters used to remove regional effects is different from the type required to filter local anomalies. Still other types can be designed to filter out anomalies of intermediate dimensions. None of these filtering operations perfectly separate desired anomalies from undesired once, but they have to be quite useful for bringing features of interest in to clearer focus.

3.7.5. Polynomial Fitting Trend Surfaces (Methods of Least Squares)

This is purely analytical method; in which matching of regional by a polynomial surface of lower order exposes the residual features as random errors. The treatment is based on a statistical theory. In practice the polynomial is rarely extended beyond the second order. In any case

the operation requires a computer and is somewhat formidable.

The regional is sometimes represented by a low order analytic surface. The parameters of the analytic surface are usually determined by a least squares fit (Agocs, 1951) or some similar operations. How closely the surface fits the data depend on the order of the surface and the magnitude of the area being fitted. Nettleton (1976) illustrates orders of fit for a one-dimensional case. The regional surface often that given by a polynomial or the low order components of a 2-D Fourier surfaces. The selection of orders usually made by examination of trial fits of several different orders.

Surface fitting is sometimes done to isolate and emphasize trends. Results from Coons, Wool, and Hershey (1967) verify that the trend becomes more evident as the order increases up to some point, about tenth order for the data they examined. The residual for low order still contains appreciable regional trend and thus low orders are not very effective in separating the regional from the residual. Like wise, high order surfaces are not effective because much of the sought-after anomaly is mixed with the regional in the surface fit.

CHAPTER FOUR

GPS _SURVEY DATA

In order to describe the position of gravity data, the GPS survey was taken in conjunction with the gravity acquisition. These data have been used to locate and orient the gravity stations besides, appertaining to the gravity data reduction. In actual field survey, 406 GPS data were recorded over the detail Omo grid (see figure 5-1). That is, the GPS was required over a grid rectangular pattern on a km inter station separation on nine, 48 km long gravity traverses, 4km a part in the survey area of the Omo Basin. The Trimble GPS survey program have been available for processing the GPS data and therefore, the final adjusted co-ordinates of the 406 gravity stations are produced in the WGS-84 reference datum with appreciable over all precision; 0.02946 m in the vertical direction and 2.97852 E-9 rad in latitude.

4.1 Instrumentation

The Omo Basin GPS survey employed Trimble 5700, Leika 500 and Top Con GPS + instruments with their complete kit requirements. It is known that these instruments provide higher degree of accuracy and productivity not only due to their ability to track both low and high frequency of all the 24 GPS satellites, they can also receive the signals from 9 GLONASS positioning satellites found of the Global Navigation Satellite System (GNSS).

The GNSS is composed of the GPS and GLONASS positioning satellite networks. The satellites transmit radio signals at known wavelength and time. Two sets of signals are transmitted from each satellite, one long

wavelength (low frequency) and the other short (high frequency) to provide a precise position in a designed datum.

The above mentioned instruments can receive both signals from the satellite and hence they are by far better than those the conventional engineering GPS survey instruments for they give rise to a highest degree of precision. This instrumentation therefore helped this study to have accurate and precise data.

4.2. Methods And Techniques In The Gps Survey

In GPS survey, different methods and techniques could be used to achieve the desired goal designed for a particular survey area. In line with the particular interest of this study, the most accurate methods and techniques that can be applied to derive the positions of the gravity stations with appreciable accuracies were employed. To state, a Static, a Fast static methods were utilized, as consequence a vector between two stations relative to the center of the earth was determined for this study in WGS-84 datum. A reference base station with known position was also established. It should be known that the accuracies of the coordinates derived with in the survey area are depended on the accuracy of this reference coordinates.

Two sets of GPS instruments with a potential to receive both the low and high frequencies from the GNSS were employed to receive radio signals at the base /control station (known position) and roving station (unknown position) through a base and mobile GPS receivers respectively.

Static GPS surveying method was applied with a static occupation at a base and/ or control where a base GPS receiver based and loged data for an appropriate amount of time to obtain the required accuracies. On the

other hand, the Fast static method was accomplished with a very short fast static occupation where by, the rover GPS receiver kit was set up over the first of the new control and/ or intermediate stations (unknown points) so as to log data for a time as little as 8 minutes, which is a modified form of a static mode.

There fore, the GPS survey data of the Omo Basin study was collected through static and its modified form – a fast static method. Un like the real time surveying method, as post processed and no radio were involved, the two tools made the study to come up with more accurate data. How ever, with no compromise, the two are the most time consuming and expensive parts in a gravity survey. Nonetheless, these are the only practical tools to determine measurement of vertical position (z) better than ± 1cm + 1ppm for a time as little as 5-20 minutes fast static occupation. More over, this accuracy is required to determine Bouguer gravity anomaly (ρ =2.67 g/cm^3) precision with in 0.001 mgal.

FIGURE 4.1: GPS CONTROL NETWORK

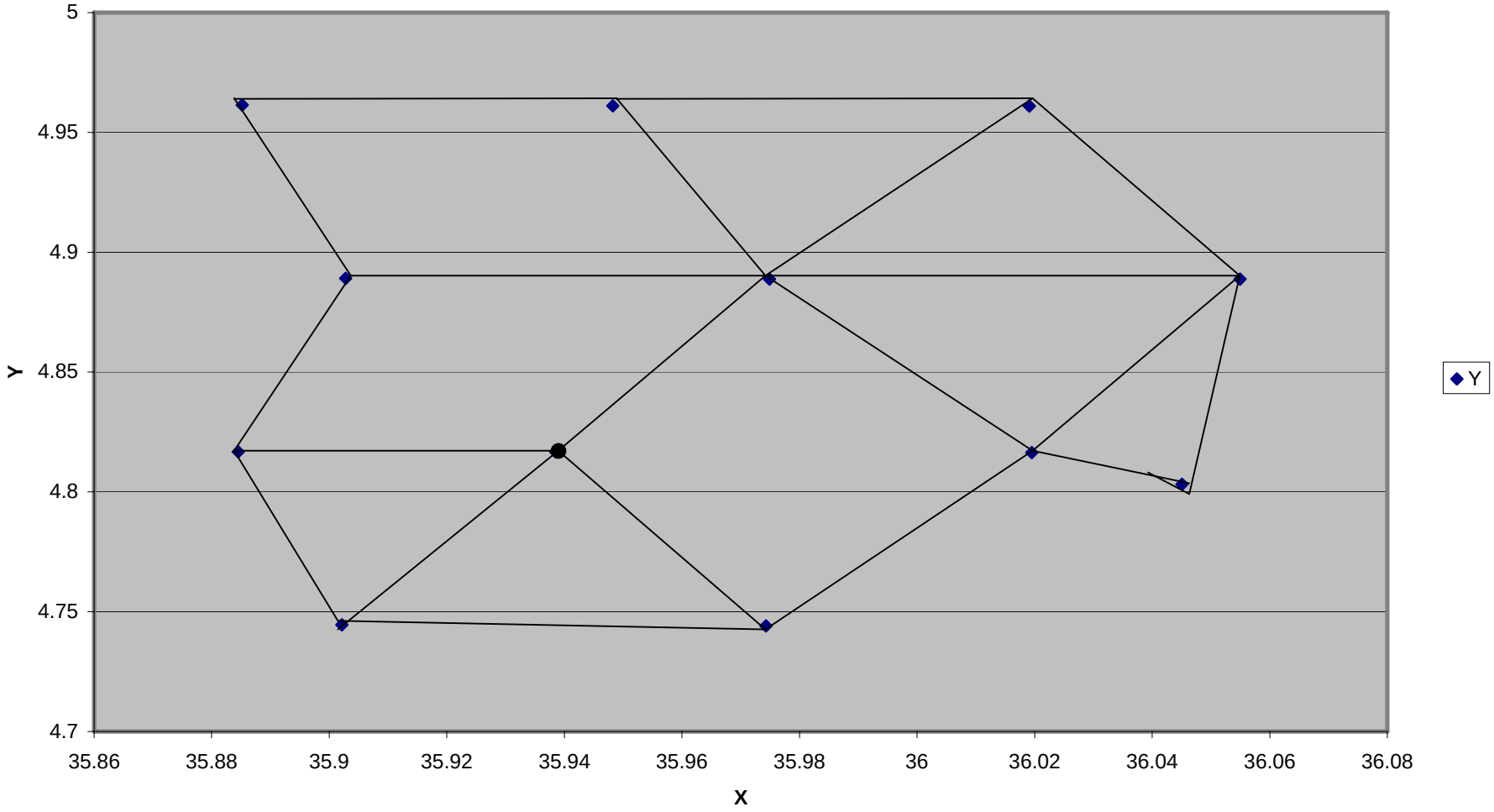

4.3. Carrying out the Survey

Base benchmark was established in the Eastern bank of Omo River, which was named and known here after as station I.D.BME. The location was adopted depending on the standard GPS surveying guidelines. Hence, a care was taken to: ensure safer, secure and accessible location; to make the location open to the sky as far as possible; and to avoid proximity to telecommunication masts or stations and power lines and pylons. In accord with the guidelines a care was also taken into consideration while a station reconnaissance for a control station was established.

Static occupation at BME with precise certainties and an occupation time of 18 hours was used to obtain an absolute WGS-84 position. This survey was repeatedly carried out for successive three days to improve the accuracy of the absolute position by averaging reducing values. With the completion of processing using GPS survey Trimble Wave Processor, the absolute position (latitude, longitude, ellipsoid height) and its estimated error were obtained. BME with measured values of WGS-84 coordinates was used for reference base where upon control stations were made to tie the Omo Basin GPS- survey to a common reference frame. To mention, other tying control stations were established from the BME at every 8 km static occupation of 8-20 minutes.

The Western Omo Basin GPS survey control network built over the actual Omo Basin grid is depicted in Fig.4-1. This network was setup based on the following two criterions as often supported by the theory:

- The network made to be close mathematically and geometrically.
- The sum of the squares of the residuals made to be minimum.

After the control stations were established, Fast Static surveying was commenced for each intermediate gravity stations. Everyday operation was performed with one Trimble 5700 set base over a control station in a static mode to log a static data for an allotted amount of time while the other Trimble 5700 set rove over the first of the new intermediate gravity stations planned to be surveyed with 8 minute fast static occupation assigned for each station.

4.3.1. Gps Data Quality Control

The daily GPS data was evaluated according to the basic GPS data quality control and assessment criterion stated below:

I. Less than ± 5cm, i.e., one standard deviation station – to – station and relative to the established control with in the area, which gives 95% confidence interval that all data points collected were repeated to be better than ±10cm i.e., equivalent to two population standard deviations.

II. Those stations that up on reoccupations showed differences in the coordinates that fall out side the two standard deviations were routinely repeated. The position error was emanated from the base lines i.e., distance between the roving and base GPS receivers relative to the center of the earth as modeled by WGS-84 mathematical ellipsoid up to 8 km.

4.3.2. Occupations Made in the Field

The satellite stations were checked to make sure the availability of enough satellites (greater than four) and the PDOP value was suitable (less than five) at the time of data logging. Furthermore, elevation mask was taken care of 15 degree for fast static applications.

4.3.3. The Operation of the Base Receiver

The base GPS kit over a control station was set and connected the base GPS Trimble receiver to the Trimble antenna on a tripod, then, to the field controller (TSC1) and the power of the turned on. The status information for the number of satellites tracked (>5), the PDOP mask (<5) and elevation mask (15^{o}) was checked. The base station survey was begun and in the mean times the necessary and the appropriate details like control station I.D., antenna height, and the measurement type (true vertical) were arranged. These and other valuable information were recorded on the field notebook. The TSC1 was disconnected while the base receiver logging data for a considerable time till the rover accomplished its operating task.

4.3.4. The Operation of the Rover Receiver

After leaving the base logging static data, the rover GPS kit was positioned over the first of the new control intermediate stations. Using bipod or tripod set the field controller (TSC2) was connected to it. The status for sufficient GPS satellites (>5), PDOP values (<5) and elevation mask (15^{0}) was checked. The rover station was started and in the mean times the necessary and appropriate details like control station I.D., antenna height, and the measurement type (true vertical) were arranged. The duration and remaining time labels changed whenever data logged at

that position (station) once the necessary amount of time was elapsed (with 8 minutes fast static occupation) the logging was stopped and the rover GPS kit moved to the next control intermediate station, the whole process was repeated. It must be also known that all the necessary information pertinent to all field occupations was recorded in the field data book.

4.4. Processing Gps Survey Data

The GPS survey data of this study is processed depending on the GPS survey program group comprising: GPS survey manager, the wave base line processor, and TRIMNET plus. These made the research to produce a final adjusted coordinates in a WGS-84 datum. Besides, daily data logging and base line processing of all GPS surveying was taken place.

To mention, the following basic tasks were accomplished in the daily GPS processing:

I) Data logging

- All log files were downloaded from both the rover and base Trimble GPS receivers.
- Occupations made in the field were reviewed in accord with the daily information recorded on the field data book.
- Fixed control coordinates were entered for static occupation(s), control base line solution have been already found by processing data logging from the control stations surveyed with fixed BME coordinates.

II) Base line processing

This task was performed using the base line processor called WAVE (Weighted Ambiguity Vector Estimator). More over, WAVE processor was helpful in evaluating the data quality based on the quality control parameters displayed for a base line solution in combination with Loop Closure in the GPS survey control network. Both concurred to make the final decision on accepting questionable results.

III) Base line solution

With the completion of processing the base lines using WAVE processor, results from a base line reduction scenario were accessed. Solution summary describes a terse list of base line results. A base line is represented by a line summary. For each solution: from- and to station names, base line length, the solution type, ratio for fixed solution and the reference variance. Of particular concern here is result quality, the last three quality indicators have been examined carefully.

Depending on these solutions that were found to have float solution type were routinely repeated. The questionable results due to low ratio and high reference variance valleys were also evaluated to make final decision either to accept or reject their values.

More over, before decision was made to accept the processed data as a reliable or unquestionable, further quality control solutions were applied. These are fixes solution type, a ratio generally greater than 1.5 and a reference variance less than 10. As to the ratio is concerned, higher number is preferable for it leading to accurate results. Where as, in the reference variance, a number greater than 10 is highly suspected. In

general, the ratio and the reference variance threshold values were considered based on Fisher's and Chi-Squared distributions at 95% level of confidence respectively.

To sum up, Omo Basin GPS data results confirm that all solutions are fixed. All the ratios are over 10.5 and most of the reference variance are reasonable only with few exceptions of greater than 10. The perfection in the results stems from the strict follow up made during the data collection and processing activities in addition to an exhaustive effort exerted to avoid problematic data through repeated measurements.

CHAPTER FIVE

DETAILED GRAVITY DATA ACQUISITION

Scintrex portable Model CG-3, and Lacoste and Romberg Model G-1105 land gravimeters were employed for the gravity data acquisition over the detail Omo Basin grid (Figure5.1). They are stable, accurately thermostated (Controlled at 54C°) and metal clamped modern gravimeters, which measure a relative gravity with respect to a gravity base; besides, they have a worldwide range with out resetting.

Gravity survey was conducted based on a station number scheme in which all gravity stations have defined and unique number over the detailed Omo Basin grid .the station number was used to describe a station and to look up other relevant information which might be determined separate from gravity survey as the GPS data .The gravity data collected during daily survey have been recorded in the field data book and have comprised station number, gravimeter reading, ground location, and terrain parameters.

At the end of the daily survey the collected data were fed to PC and their accuracies were assessed such that loops incorporating gravity stations up on reoccupations show differences in the measured gravity that fail outside two standard deviations. i.e., ± 0.1mgal were routinely repeated. A total 406 gravity data with the required accuracy have been collected in gravity loops, which started and ended at either of gravity bases, and sub –loops derived from reoccupations at sub – gravity bases at intervals of 2 –3hours. Gravity “loop” has the first and the last gravity measurement on a known gravity base, with any number gravity measurements in

between. There can be sub- gravity base (s) located within a loop to create sub –loops.

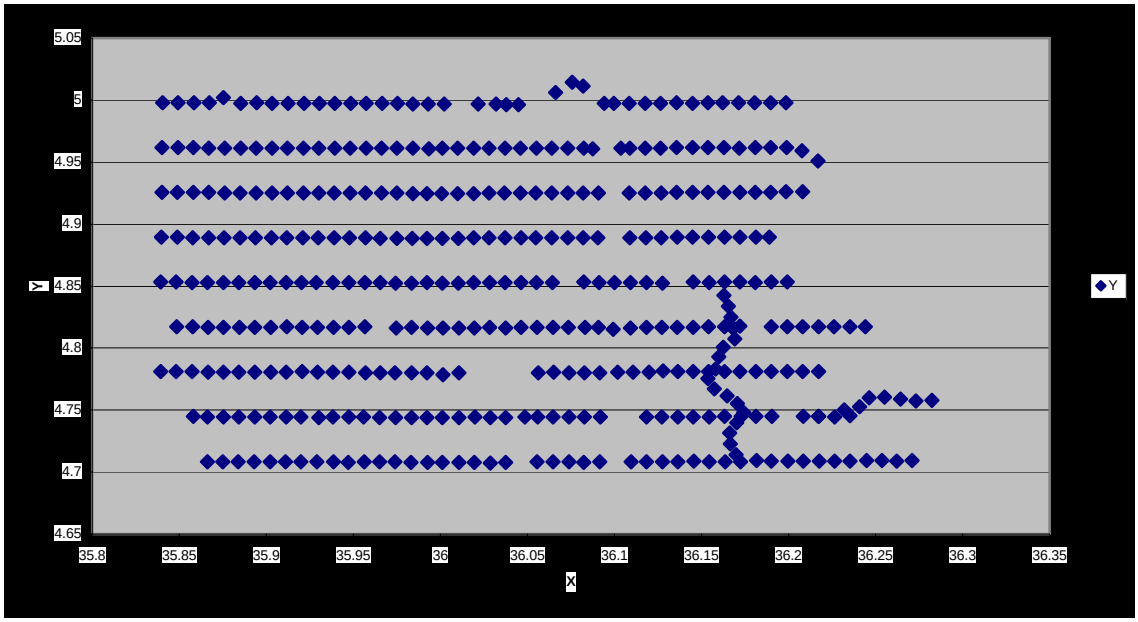

Fig. 5.1: OMO BASIN grid.

5.1. Gravity Base

Gravity survey is conducted by starting and ending at a station with a known reference absolute gravity value. This station is called a gravity base. The reference absolute gravity value at a gravity base is normally being established by separate gravity base survey. Thus, a reference absolute gravity value $\mathbf{g_r}$ at a base, established for particular gravity survey, is normally found with ties made to the IGSN -71 stations. However, if none of this station is found in proximity, it may be

necessary to determine the reference absolute value of gravity using gravimeter measurement adjusted to the IGSN-71.

Gravity base survey is carried out like normal gravity survey except that all occupied stations are bases. The first and last occupation must be gravity base/station, which has been referred to the IGSN –71-gravity datum. The gravity base survey can be repeated multiple times to improve the accuracy of the reference absolute gravity by averaging reducing values. It may be required more than one gravity base, so that gravity base survey can be conducted to establish other gravity bases. A gravity base station comprises station name, absolute gravity and coordinates.

5.1.1. Omo Basin Gravity Base

Two gravity bases have been established and have comprises a substantial and robust concrete platform in the position that will have minimized the possible damage in the next few years. Therefore, these bases will have a significant contribution for gravity studies and ties with in – and in the proximity of the area. Separate gravity ties have found their absolute gravity values. Gravity base surveys were conducted separately between Omo basin gravity bases and an existing Omorate gravity base (977907.94mgal), which has been referred to IGSN-71gravity datum. Omorate gravity base was reoccupied at short interval of 1 hour for eastern gravity base survey and 2 hour for the western one in order to control drift-tide effects. These surveys were repeated three times to improve the accuracy of the absolute gravity values by averaging reducing values. Data collected at each occupation included relative gravimeter reading, reading time and date. In addition, WGS –84

coordinates of each gravity base were obtained from a separate GPS-survey.

5.1.2 Absolute Gravity at Gravity Base

Absolute gravity values of Omo Basin gravity bases referred to the IGSN-71gravity datum were calculated as follows:

Dial reading are converted to relative milligal values based on a user supplied calibration table of the La -coste and Romberg gravimeter Model G-1105; Relative gravity milligal values (scale corrected readings) were corrected for earth tides due to the position of the sun and the moon at the time and location of the observation (reading). A computer program (Oasis motaj Geosoft, 2003) was availed on computing tide variation provided relative time difference to Greenwich Mean Time (GMT), i.e. -3hour;Each base reading was corrected for the height of the instrument hi=0 above the station or base at which elevation was measured.

$$\delta_i = 0.308596\ hi \qquad (5\text{-}1)$$

Where, δ_i is instrument correction.

Adrift was calculated base on rate of drift variation between the first and the last tide and instrument height corrected relative milligal base value in each loop;

Finally, equation (3.44) in conjunction with (3.45) was used to obtain the absolute gravity values. Thus, by combined the value of g_r Omorata

gravity base (977904.94mgal) and the gravity difference Δg between this and of the Omo gravity bases, their absolute gravity values referred to the IGSN –71datum were calculated.

Accordingly,

$$g = g_r + \Delta g \qquad (5\text{-}2)$$

$$\Delta g = \delta g_{E/W} - \delta g_{r,} \qquad (5\text{-}3)$$

Where, $\delta g_{E/W}$ is relative milligal value either east or west Omobasin gravity base and δ_r is that of the reference Omorate base .

The OmoBasin absolute gravity base values are g_{BEO} (977907.821mgal) and g_{BWO} (977907.839 mgal) in the IGSN-7 1datum.These have been determined in consistent with the aforementioned computations.

5.2. Detailed Gravity Station

5.2.1. Gravimeter Occupation

Gravity measurements over the detailed Omo basin grid was performed well at reasonable sequences of field survey loops and sub- loops for drift –tide control along the traverse lines, in which gravity base was occupied three times early in the day with a maximum duration of 3 hours for a trip. Sub- loops were then made along the traverse line where up on a station within a sub-loop was reoccupied every 2 – 3 hours or less to create successive sub–loops. Hence, gravity sub-bases are established in sequences there. Final measurement was taken at gravity base such that each gravity loop was begun and ended at gravity base with maximum interval of 12 hours. In addition, these gravity sub- loops are taken care of estimating the measurement precision as outlined in section 6.2.

5.2.2. Terrain Observation

Clinometers measurements were taken in the field data acquisition session for Hammer zones B, C and D where local terrain in proximity of gravity station exceeded 5 degrees according to the Hammer (1939) field observable outlined in table 5.1.

The survey area is reasonably flat, which were rarely required rough topography around a gravity station and hence, terrain observations were taken for a total number of 34 gravity stations. Terrain corrections were calculated for these gravity stations using terrain Formula (3.54) described in section 3.5.4; Chapter3.

Zone	Compartment	r_i(m)	r_o(m)
B	4	2.0	16.6
C	6	16.6	53.3
D	6	53.3	107.3

Table5.1 Field observation for Hammer zones; r_i(m) , r_o(m) are the radii of the inner and outer rings bound

5.2.3 Absolute Gravity At A Gravity Station

The measured relative gravimeter readings between gravity stations and IGSN –71 gravity base (either BEO or BWO) or each sub- gravity base in which their absolute gravity is calculated from successive ties with gravity base, were incorporated to calculate the absolute gravity values at the ground locations. In general a total of 406 gravity stations were referenced to the IGSN-71datum in accord with procedures stated below

a. Calibration scale factor

The calibration scale factor converts a reading to a relative milligal value based on a calibration table. In the present work, it was derived from users supplied calibration table for G-1105 of the La –coste and Romberg ModelG-1105 land gravimeter. Mathematically this may be written as:

$$\delta g_c = \delta R_{VH} + \delta R_F \text{ © } C_F \quad (5\text{-}4)$$

And,

$$\delta R_F = \delta R - \delta R_H \quad (5\text{-}5)$$

Where,

δg_c Relative gravity miligalvalue

δR_{VH} Value in milligals for the multiples of thundered –reading

δR_F Fraction reading in dial units

C_F Milligal correction for the fraction (milligal /dial units)

δR gravimeter reading in dial units

δR_H multiples of hundred –reading dial units

b. Tide correction

All Omo Basin grid readings were corrected for earth tides due to the position of the sun and the moon at the tine and location of observation. Thus, computer program, Oasismotas Geosoft (2003) used for calculating tidal variations of gravity provided relative time differences to Greenwich Mean Time (GMT), i.e. -3hours

c. Instrument height

Each reading was corrected for the height of the instrument above the station or base at which the elevation was measured. Null instrument height was applied for all measurements

$$\delta g_h = \delta g_t + 0.308596\ hi \qquad (5\text{-}6)$$

Where δg_h , instrument height corrected relative gravity; δg_t , tide and scale corrected relative gravity from 2; hi, Instruments height in meters.

d. Drift correction

A drift was calculated based on rate of drift variations between the first and the last reading in each sub –loop

$$D = (\delta g_{h2} - \delta g_{h1})/ (T_{l2} - T_{l1}) \qquad (5\text{-}6)$$

Where D, drift in mgals per hours ; T_{l1}, T_{l2} ,first and last sub- base reading time ,respectively; δg_{h1},δg_{h2} First and last sub-base relative gravity in each sub-loop , tide and instrument height corrected .

e. Absolute gravity

The absolute gravity at a station g was computed by combining equations (3.44) and (3.45) .

Evidently, all these formulas were properly applied and therefore the Omo Basin absolute gravity values at 406 gravity stations have been obtained at a worldwide distribution of gravity stations, henceforth, gravity stations are referenced to IGSN-71 datum.

CHAPTER 6

OMO BASIN GRAVITY DATA

6.1 Gravity Data Organization (Preparation) And Processing

As it was described in chapters four (GPS data) and five (detail gravity data) a total of 406 gravity values with reference to the IGSN-71 datum and their corresponding WGS- 84 positions have been obtained form the field data acquisition session covered the period from 2nd February to the 7th April 2006 of the Omo Basin area, Southern Rift Basins, Ethiopia. In addition, corrections for gravimeter drift and earth tide were made in a steady purpose to obtain accurate values of absolute gravity. Conveniently a total number of 406 gravity stations are found over the detail Omo Basin grid for contemplated processing and interpretation to draw valuable geological information, of the Omo Basin.

The gravity stations, 406 in number, were referenced to the International Gravity Standardization Net 1971 (IGSN-71) datum and the reference ellipsoid is the Geodetic Reference system 1967 (GRS67).

The gravity values observed on the actual topography of the earth's surface are properly reduced to their respective positions on the geoid surface by applying the standard components of gravity reduction. These could have allowed for reasonable computations of gravity anomalies in compared with the reference ellipsoid.

Moreover, several types of gravity anomalies are determined based on the decision involved in these components of reduction and here, the usual reductions as for latitude, elevation and /or terrain were made to reduce the gravity values to corrected observed gravity ,Free-air, Simple

Bouguer, and complete Bouguer gravity anomalies tied to the International gravity Network.

The geodetic Reference system 1967 (GRS 67) notified by equation (3.42) outlined in section 3.3.3 (chapter three) has been used through out the computation of the theoretical gravity at station location on the earth's reference ellipsoid. To mention, the force of gravity with latitudeΦ, on the reference ellipsoid can be approximated with in 0.1 mgal by the G RS 67 formula,

$$g(\varphi)_{1967} = \{\, 978031.846\ [\ 1+0.005278895 \sin^{2}(\varphi) + 0.00002346 \sin^{4}(\varphi)\ ] \,\} \text{ mgal} \qquad (6\text{-}1)$$

(Sheriff, Encyclopedic Dictionary of Exploration Geophysics 2nd Edition, 1984 p141)

The free air gravity anomalies were calculated using modified version of formula expressed in Equation (3.58) section 3.6.1

. i.e., given by:

$$\Delta \mathbf{g_F}(\mathbf{g},h,\Phi) = \{\, \mathbf{g} + [0.308767763-0.000439834 \sin^{2}(\Phi) - 0.000000072124602h]h-\mathbf{g}(\Phi)_{1967} \,\} \text{ mgal} \qquad (6\text{-}2)$$

(Heiskanen and moritZ, 1967, physical geodesy: Sanfransisco, Free man Press)

Where g (Φ) is the GRS 67 theoretical gravity (6-1) on earth's reference ellipsoid, at latitudeΦ.**,** and geodetic height **h**, in meters.

The complete Bouguer gravity anomalies were calculated from the free-air gravity anomalies using the Bouguer reduction, terrain corrections, and reduction densities of 2.2, 2.4 and 2.67 grams/cm^3. Thus,

$$\Delta g_{C\text{-}B}\,(\,g,h,\Phi\,,\,\rho\,) = [\,g + \Delta g_F\,(g,\,h,\Phi\,) - \delta g_B\,(\,\rho,h\,) + \delta g_T\,]\ \text{mgal} \qquad (6\text{-}3)$$

Equally,

$$\Delta g_{C\text{-}B}\,(\,g,h,\Phi\,,\,\rho\,) = [\,g + \delta g_F\,(\,h,\Phi\,) - \delta g_B\,(\,\rho,h\,) + \delta g_T \;-\; \mathbf{g}\,(\Phi)_{1967}\,]\ \text{mgal} \qquad (6\text{-}4)$$

Where $\Delta g_F\,(g,\,h,\Phi\,)$, Free-air gravity anomaly from (6-2) ; $\delta g_B\,(\,\rho,h\,)$, Bouguer reduction from (3.50) ; δg_T, terrain correction as verified here below.

The topography is reasonably flat; terrain corrections were required for only a number of gravity stations. The area comprise rarely rough terrains, hence only 34 gravity stations necessitated local terrain corrections that reached amplitudes of 0.2- 0.41 mgals. Average densities of the sub-surface were taken to be 2.2, 2.4, and 2.67-grams/ cm^3 and these were used in computing the Bouguer and terrain corrections.

The terrain corrections were applied using Hammer (1939) tables and were considered accurate with in 0.01 mgal.

The accuracies of measured gravity, elevations and latitude determinations were assessed for the errors introduced to the computed complete Bouguer gravity anomalies using the schema described in Section (6-2). The average elevation, measured gravity and station latitude uncertainties in this survey were estimated to be ± 0.026m, ±

0.036mgal and ± 5.25 E-9 radians, respectively derived in section 6.2 which translate in to uncertainties in the combined free- air and Bouguer reductions of approximately 0.2-0.21 mgal. Beside observed gravity that amounts to ± 0.036 mgal and its corresponding theoretical, value± 0.4 E-9 mgal. The r m s errors/ the over all accuracies of the complete Bougue gravity anomalies were estimated at ± 0.03827,± 0.03802, ± 0.03794, for average densities of 2.2, 2.4 and 2.67- grams/ cm^3, respectively with underlying assumption that correct sub-surface densities have been consisted. The analytical error analysis is taken care of the next portion.

6.2 Bougver Gravity Anomaly Accuracy

The accuracies of the measured values determinations were assessed, evaluated and computed for the errors introduced in the computed complete Bouguer gravity anomalies, as presented here below.

The measured elevation, gravity, and latitude uncertainties were estimated separately to determine the combined effect of the standard (random) and systematic (bias) errors translated in the computed complete Bouguer gravity anomaly. Practical assumption underlying this approach was that all blunders (slip-up) errors have been eliminated from the field observation.

The task is accomplished in accordance with the C- Bouguer gravity anomaly Formula wherein these measured parameters are consisted, i.e.

$$\Delta g_{C\text{-}B}\,(\,g,h,\Phi\,,\,\rho\,)\;=\;[\;g\;+\;\delta g_F\,(\,h,\Phi\,)\;-\;\delta g_B\,(\,\rho,h\,)\;+\;\delta g_T\;\;-\;\;\mathbf{g}\,(\Phi)_{1967}\,]\qquad \text{mgal}$$

(6-4)

The approximation with the standard components of reduction:

$$\Delta g_B (g,h,\Phi, \rho) = [g + 0.30859h - 0.04198088\rho h + \delta g_T - \mathbf{g}(\Phi)] \text{ mgal} \quad (6\text{-}5)$$

The over all mean square error $\sigma_{\Delta g}$ of the complete Bouguer gravity anomaly is defined by

$$\sigma^2_{\Delta g} = R^2_{\Delta g} + S^2_{\Delta g} \quad (6\text{-}6)$$

Where, $R_{\Delta g}$ is the standard error, and $S_{\Delta g,}$ the systematic error of the computed Bouguer anomaly.

The variance $R^2_{\Delta g}$ can be derived from the law of propagation of errors for uncorrelated measurements with an ease as follows.

Obviously, the Bouguer gravity anomaly formula (6.5) is a function of the parameters gravity **g**, station elevation h, reduction density ρ, and the station latitude Φ,so that it can be written in implicit functional form.

$$\Delta g = \Delta g (g, h,\Phi, \rho) \quad (6\text{-}7)$$

And, the differential of Δg is expressed as

$$d\Delta g = (\partial\Delta g / \partial g)dg + (\partial \Delta g \partial / h)dh + (\partial\Delta g / \partial\Phi)d\Phi + (\partial\Delta g / \partial\rho)d\rho = R_{\Delta g} \quad (6\text{-}8)$$

More progressively,

$$R_{\Delta g} = (\partial\Delta g / \partial g)\, r_g + (\partial \Delta g \partial / h)\, r_h + (\partial\Delta g / \partial\Phi)\, r_\Phi + (\partial\Delta g / \partial\rho)\, r_\rho \quad (6\text{-}9)$$

$$\Rightarrow R^2_{\Delta g} = (\partial \Delta g / \partial g)^2 r^2_g + (\partial \Delta g \partial / h)^2 r^2_h + (\partial \Delta g / \partial \Phi)^2 r^2_\Phi + (\partial \Delta g / \partial \rho)^2 r^2_\rho \quad (6\text{-}10)$$

Where r_g, r_h, r_p and r_Φ are the standard errors in determining the measured values of gravity (measurement precession), the geodetic elevation (elevation error), the reduction density (density error) and latitude (latitude error) of a station, respectively.

The standard error $\mathbf{r_g}$ can often be estimated by controlling gravity measurements. Its true magnitude can be accurately estimated only by having large enough control of reoccupations. To accompany the acme, 91 control stations (s_1, s_2,... s_{91}) were assessed. In actual fieldwork 2-3 independent gravity measurements were taken on each control station, and a total of 236 independent measurements were obtained

The internal variance (Bjerhammer, 1973) of these measurements was calculated as illustrated here below in table 6.1 using the formula follows

$$r_g^2 = \{ \Sigma_{s1} v^2 + \Sigma_{s2} v^2 + \ldots\ldots + \Sigma_{s91} v^2 \} / (n-1) \} \quad (6.11)$$

Where, $\Sigma\ v^2$ the sum of the squares of the residuals at each controls station. ;n ,the total number of independent measurements ;.s , the number of (gravity) control stations.

Standard elevation error r_h and latitude error $r\Phi$

The standard elevation error r_h and latitude error $r\Phi$ were estimated by examining GPS control stations. To accomplish the estimations, a control stations (s_1,s_2..... s_{91}) where by 2 independent measurements were recorded at each control station. thus, a total of 16 independent measurements were taken care, with ease the standard elevation and latitude errors were calculated in accordance with Equation(6-11) and their values were found to be $\pm$0.029458919 m and 5.1985 E-9

Radians, respectively. These are illustrated here above in tables 6.2 and 6.3 In addition; closure errors obtained from the GPS survey control network built maximum closure errors of values 0.027 m and 10.399E-9 radians are summed for the elevation and latitude errors in order. Thus, the following values were adopted

- Maximum elevation error $r_h = \pm$ 0.056459 m
- Maximum latitude error $r_\Phi = \pm$ 15.5395 E-9 rad (6-12)

The partial derivative of Equation (6-5) with respect to the station elevation yields.

$$\partial \Delta g / \partial h = 0.30859 - 0.04198088\rho \qquad (6\text{-}13)$$

or with reduction densities 2.2, 2.4, 2.6 grams/Cm^3 involved in calculating the complete bouguer gravity anomalies, become, 0.21624,0.20784,0.19651 mgal/m ,respectively.

For the maximum elevation error $r_h = \pm$ 0.056459 m an error of $(\partial \Delta g / \partial h)$ r_h was introduced in the computed terrain corrected Bouguer gravity anomaly, i.e.

$(\partial\Delta g / \partial h)\, r_h$, give lire to, $\pm$ 1.1992 E-2 ,$\pm$ 1.1194 E-2 ,$\pm$ 1.0898 E-2 mgal at 2.2, 2.4, and, 2.67 grams/cm^3 in order.

The partial derivative of equation (6-5) with respect to station latitude Φ is expressed by

$$\partial\Delta g / \partial\Phi = \partial g(\Phi) / \partial\Phi \qquad (6\text{-}14)$$

For the maximum latitude, error $r_\Phi = \pm$ 15.5395 E-9 rad radians an error of $(\partial\Delta g/\partial\Phi)\, r_\Phi$ was translated in to the resulted complete bouguer gravity anomaly. This can be approximated as follows.

$$(\partial\Delta g/\partial\Phi)\, r_\Phi \approx 1/R_E \; (\partial g(\Phi) / \partial\Phi)\; (R_E\, r_\Phi) \qquad (6\text{-}15)$$

Where Re is the earth's radius and we have

$$1/R_E \; (\partial g(\Phi) / \partial\Phi) = 0.83 \sin^2 (2\Phi) \text{ mgal / Km} \qquad (6\text{-}16)$$

For the mean latitude $\Phi < 4.86\,99802440^0$ of the omobasin grid and the mean radius of the earth R_E=6371.229 Km,

$$1/R_E \; (\partial g(\Phi) / \partial\Phi) = 0.13754 \text{ mgal / Km}$$

of particular concern the omo Basin grid, the variation of in the theoretical gravity is about 0.13154 mgal for each 1Km traveled in a North-South direction. Therefore, uncertainties that amounts to,

$$1/R_E \; (\partial\Delta g / \partial\Phi)\; (R_E\, r_\Phi) = 1.366807 \text{ E-5 mgal} \qquad (6\text{-}17)$$

Hence, this value was introduced in to the C-Bouguer gravity anomaly value.

Using Equation (6-10) the total standard error $R_{\Delta g}$ of the complete Bouguer gravity anomaly is calculated with an underlying assumption that the correct density has been taken. Hence Equation (6-10) reduces to:

$$R^2_{\Delta g} = r^2_g + (\partial_{\Delta g} / \partial h)^2 r^2_h + (\partial \Delta g / \partial \Phi)^2 r^2_\Phi \qquad (6\text{-}18)$$

Therefore, make use of values calculated so far:

$R^2_{\Delta g}$ (ρ=2.2) = 1.4642 E-3 mgal

$R^2_{\Delta g}$ (ρ= 2.4) = 1.4457 E-3 mgal

$R^2_{\Delta g}$ (ρ=2.67) = 1.4392 E-3 mgal (6-19)

In computing the terrain corrected Bouguer gravity anomalies no term is neglected, hence fore, the systematic error is approximated to zero value ($S^2_{\Delta g}$) using Equation (7-6) the total mean square error $\sigma_{\Delta g}$ of the terrain corrected gravity anomaly Δg is estimated to

$\sigma_{\Delta g\ g}$ (ρ=2.2) = 3.8265 E-2 mgal

$\sigma_{\Delta g}$ (ρ= 2.4) = 3.8023 E-2 mgal

$\sigma_{\Delta g}$ (ρ=2.67) = 3.7937 E-2 mgal

To sum up, the overall accuracy of the complete Bouguer gravity anomaly (considering, the right density has been taken) is approximately estimated to 0.0379 – 0.0383 mgal.

6.3. Gravity Compilations And Presentation

The gravity anomalies data so obtained have been compiled as anomaly contour maps to draw substantial geophysical structures of the Omo Basin.

The compiled results of the Geophysical surrey are shown on the figures and enclosures included in this thesis.The terrain corrected Bouguer anomalies are presented 6-1 to 6-3 for reduction densities of 2.67, 2.4, 2.2 grams/cm^3, respectively. Wavelength filtered and isolated. as well as in separate figures and they include contour maps of:

- Residual gravity anomaly; Figure 6.4.
- Regional gravity anomaly; figure 6.5.
- Vertical derivative and horizontal derivatives; Figures 6.6, and 6.7.
- Low pass filters; 6.8, 6.9,and 6.10.
- Vertical derivatives; figure 6.6 and 6.7
- Horizontal gradient; figure. 6.8
- Low pass filtered; figure. 6.9, 6.10, 6.11, 6.13, and 6.14

In addition, the following data are consisted for survey area.

- Free air gradient map; Figure 6.15
- Elevation contour map; Figure 6.16

6.4 Gravity Interpretation

The aforementioned contour maps in figures and in enclosures are compiled according to regularly digitized corresponding data. This was performed well at 1000m-grid cell size using minimum curvature gridding algorithm. Residual contours obtained for the study area are

based on the trend surface of the regional gravity anomalies approximated using a polynomial fitting of degree 3. In addition, a vertical derivative (high pass gradient filter) was produced from smoothed terrain corrected gravity date. This removes regional trends to show rift more clearly. The magnitude of the contour interval was taken to be 0.13 mgal. The contour interval is reasonably selected based on the level of errors introduced to the computed gravity anomalies determined in section 6.2 and was estimated approximately at ± 0.4 mgal.

It has been smoothed with a 500 m non- linear space domain fitter to reduce numerous data spikes.

The Gravity anomalies so presented in contour maps are displayed in figures .The patterns of these anomalies show marked relation ships, which can provide important clues on the structural units of the survey area. Because the time allocated for this study has been so limited, the interpretation is most constrained by qualitative decisions.

6.4.1 Omo Basin Gravity Analysis

The complete Bouger anomaly maps of the araA contoured at 1-3mgal intervals are shown in figures 6.1, 6.2, and 6.3.

The terrain corrected values are mostly between -53.7and -93.7mgals as shown in fig.6.3 in which they are derived from 2.2gm/cm3 average sub surface density. The basin potential and therefore the controlling structures are observed superimposed with the regional ones. The patterns of these anomalies have a N-S trend following the Omo rift and N-W trend in west OMO sub basin consisted within Ethiopia. The controlling features are shown here by N-S patterns of variation and roughly in E-W orientation in the northern part of the western side.

The Gravity lows of the Omo rift observed on the contours trend approximately N-S between longitudes 35.9938453˚ E and 36.1366393˚ E ..In addition trends of N-W are shown in between 35.828334˚E and 35.960743 ˚E longitudes located in the southwestern part of the studied aria, which extend s in to Kenyan territory.

Properly selected filters are used for clearer focus of the omo basin potential and its controlling features besides the residuals .N-S structures are recognized by lateral distribution of anomaly patterns with ease and sharp changes in the gradient of the anomaly field (figures 6.6 and 6.7)

Although it is difficult to use the wavelength filters as depth estimation because of the effects of geometry and size of the source, cut of wave lengths to about 20 kms are taken care of the depth.

CHAPTER SEVEN

CONCLUSIONS AND RECOMMENDATIONS

The processed gravity data show an approximately N-S trending, fault-bounded Omo rift basin clearly indicated by gravity laws. The width is about 15.87048933 kms .the north-south trending ranges are clearly mapped on both sides of the basin and have been identified as volcanoclastic and basaltic sequences from their outcrop in the western part of the Omo river The basement is seen to outcrop in the eastern part in north-south direction .The regional extension direction as deduced from field observation and the processed results are east- west .the basin are later on affected by northwest-southeast trending structures and shows slight northwest offset in its northern part . The depth of the basin seems to be more than 3 Km as judged by processed results incorporated advanced filtering. It is of course essential to perform two-dimensional modeling in the central part to have a good approximation of the depth to each of the geological units.

In the southwestern part of the studied area is located a bigger and deeper and more pronounced basin which extends in to Kenya. It is essential and highly recommended to make a detail stud of the basin from Kenya side to get a better picture and understand its mode of formation.

FIG.6- :REGIONAL GRAVITY ANOMALY OF OMO BASIN

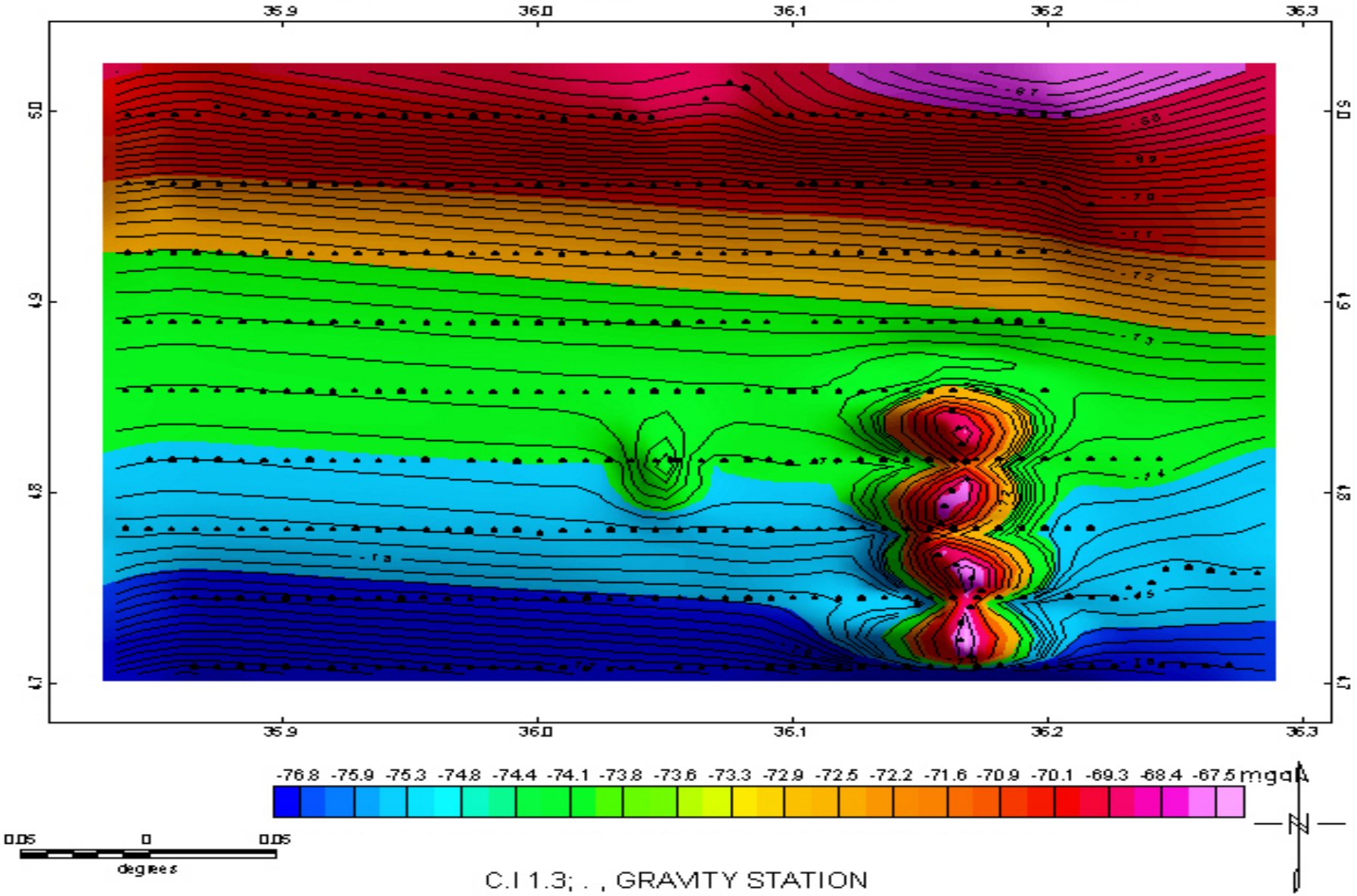

C.I 1.3; . , GRAVITY STATION
D=2.2g/cm^3

ELEVATION OMO BASIN

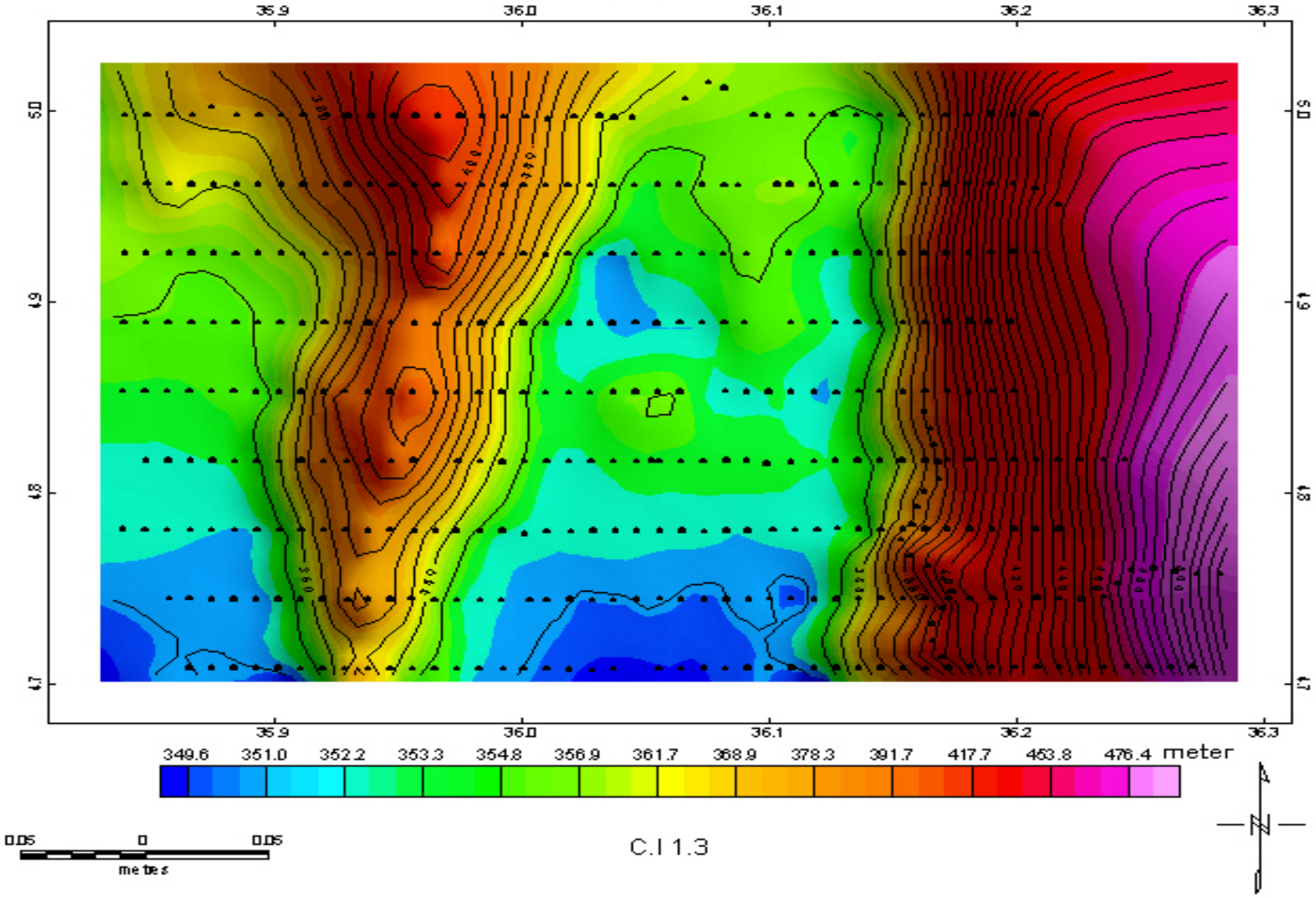

FIG.6- :FREE-AIR GRAVITY ANOMALY OF OMO BASIN

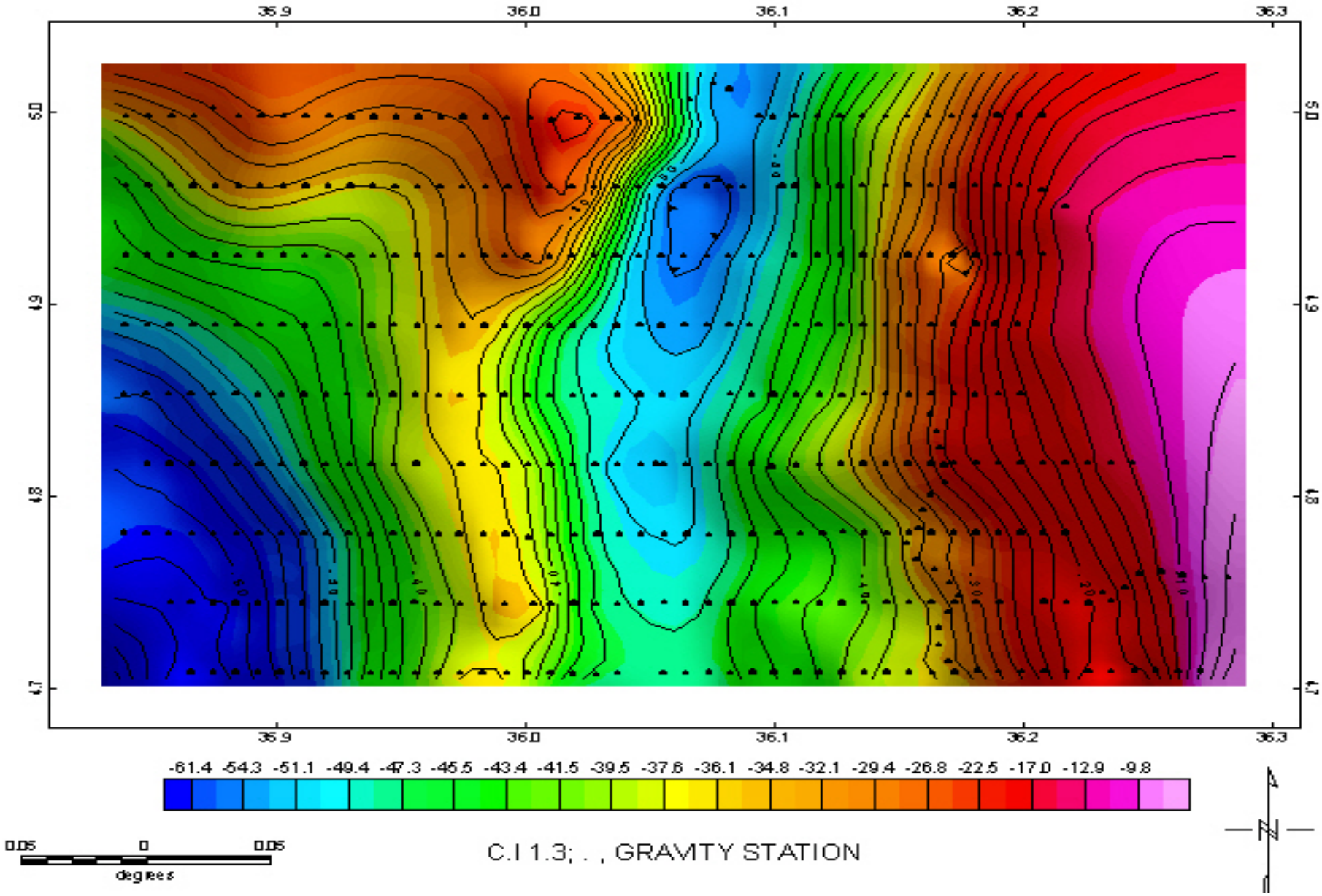

Fig.6- :HORIZONTAL GRADIENT C_BOUGUER GRAVITY ANOMALY OF OMOBASIN

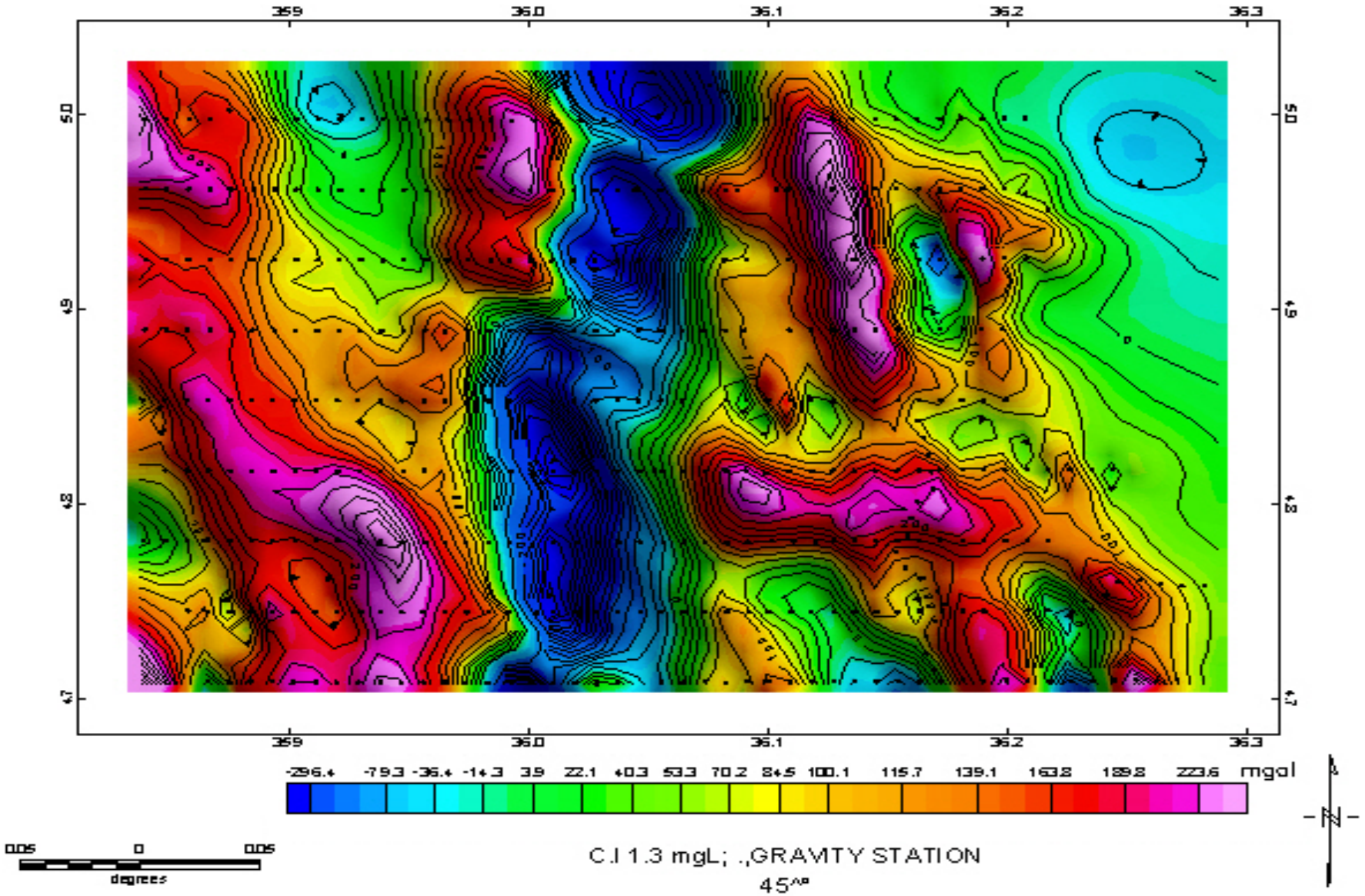

Fig.6- :LOWPASS FILTERED C_BOUGUER GRAVITY ANOMALY OF OMOBASIN

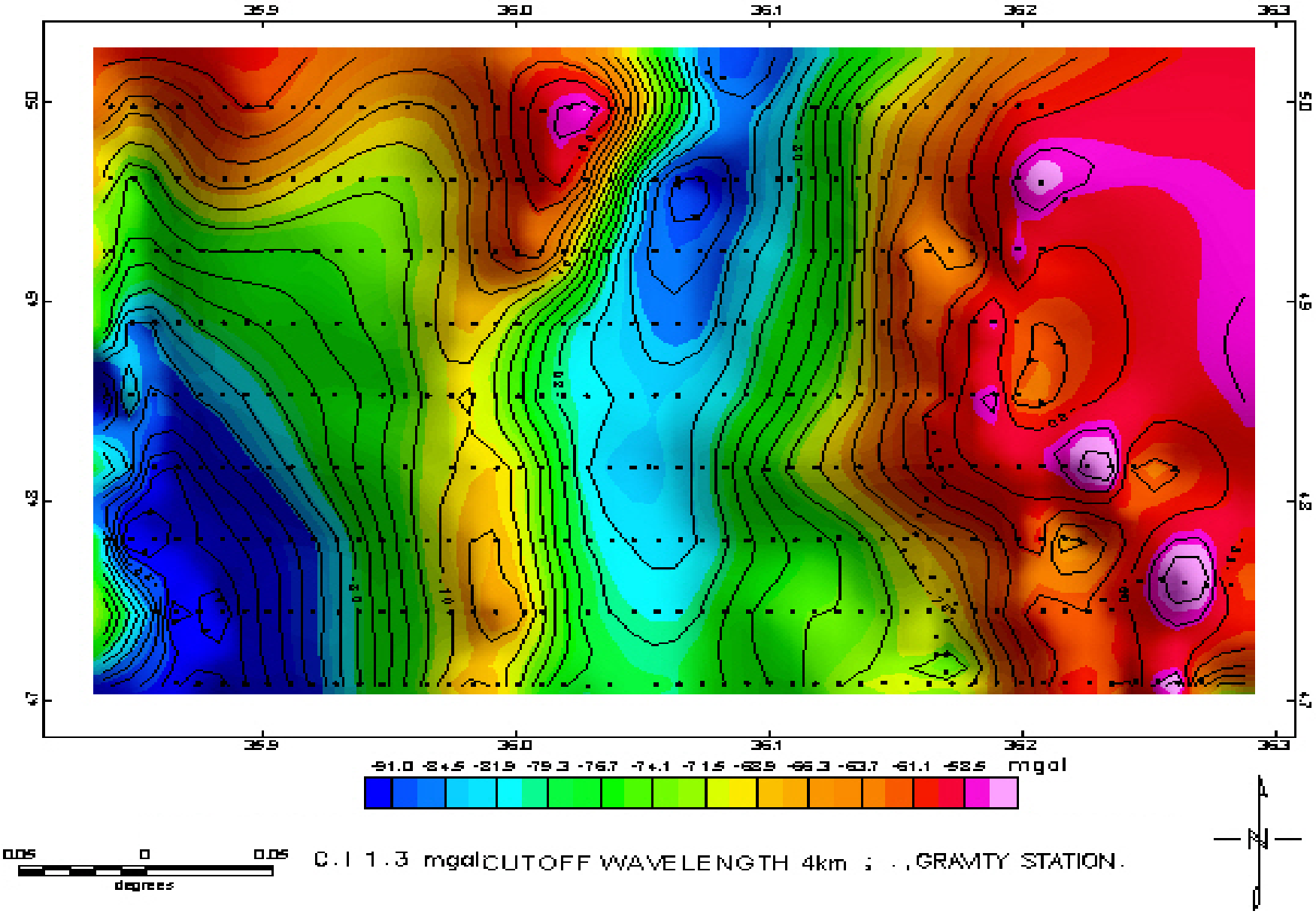

Fig.6- :LOWPASS FILTERED C BOUGUER GRAVITY ANOMALY OF OMOBASIN

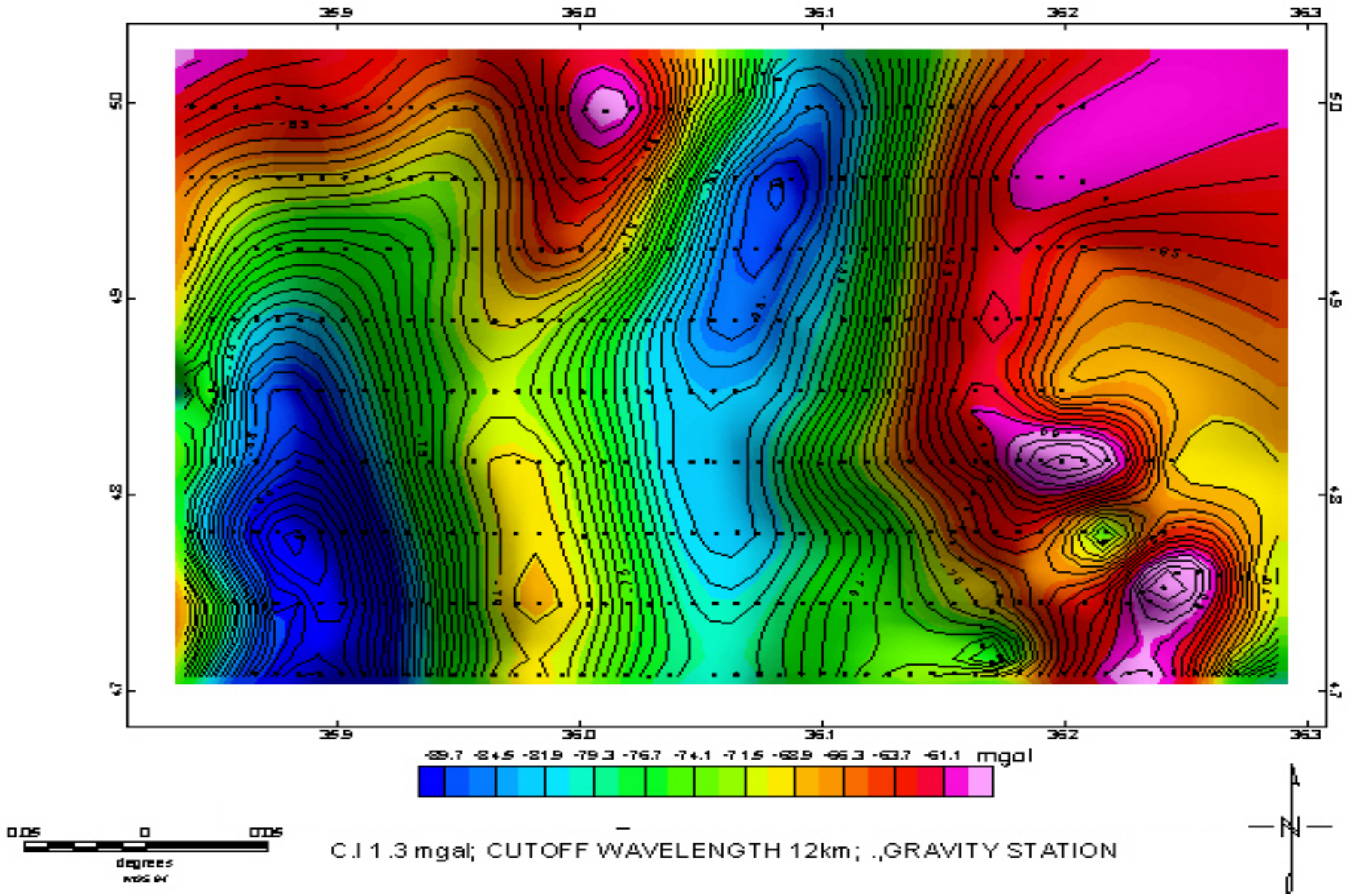

Fig.6- :LOWPASS FILTERED C_BOUGUER GRAVITY ANOMALY OF OMOBASIN

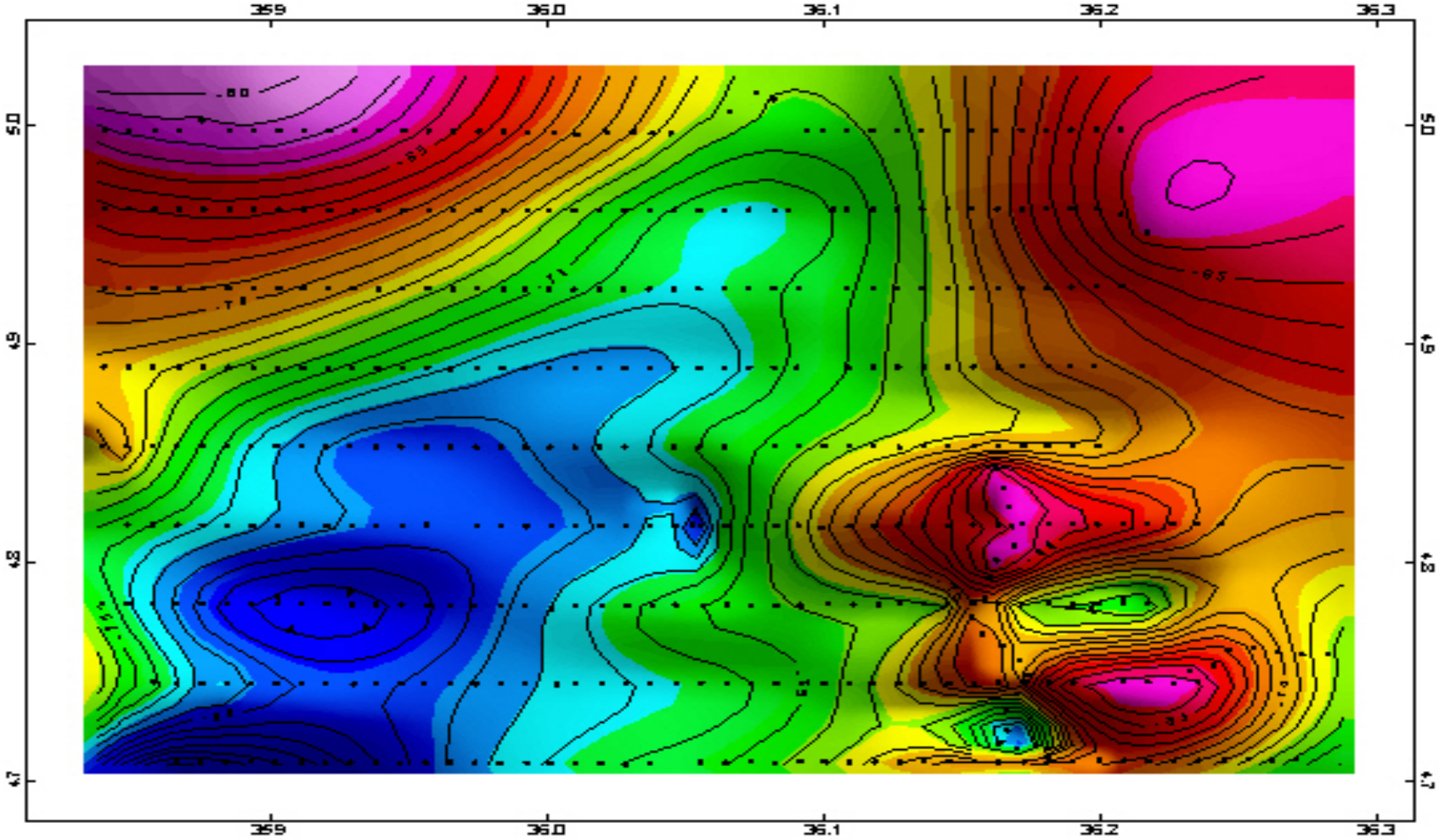

Fig.6- :LOWPASS FILTERED C_BOUGUER GRAVITY ANOMALY OF OMOBASIN

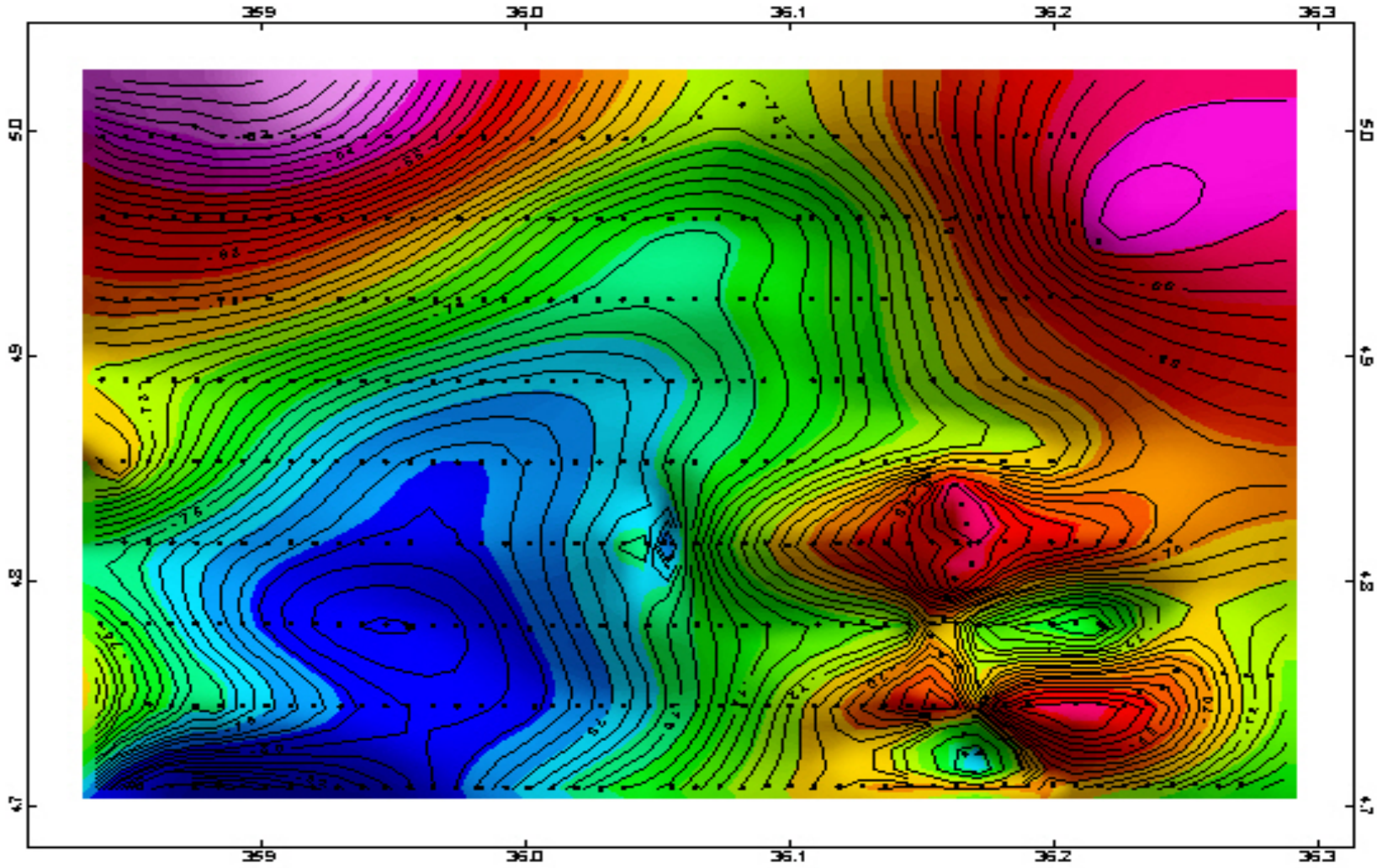

Fig.6- :LOWPASS FILTERED C_BOUGUER GRAVITY ANOMALY OF OMOBASIN

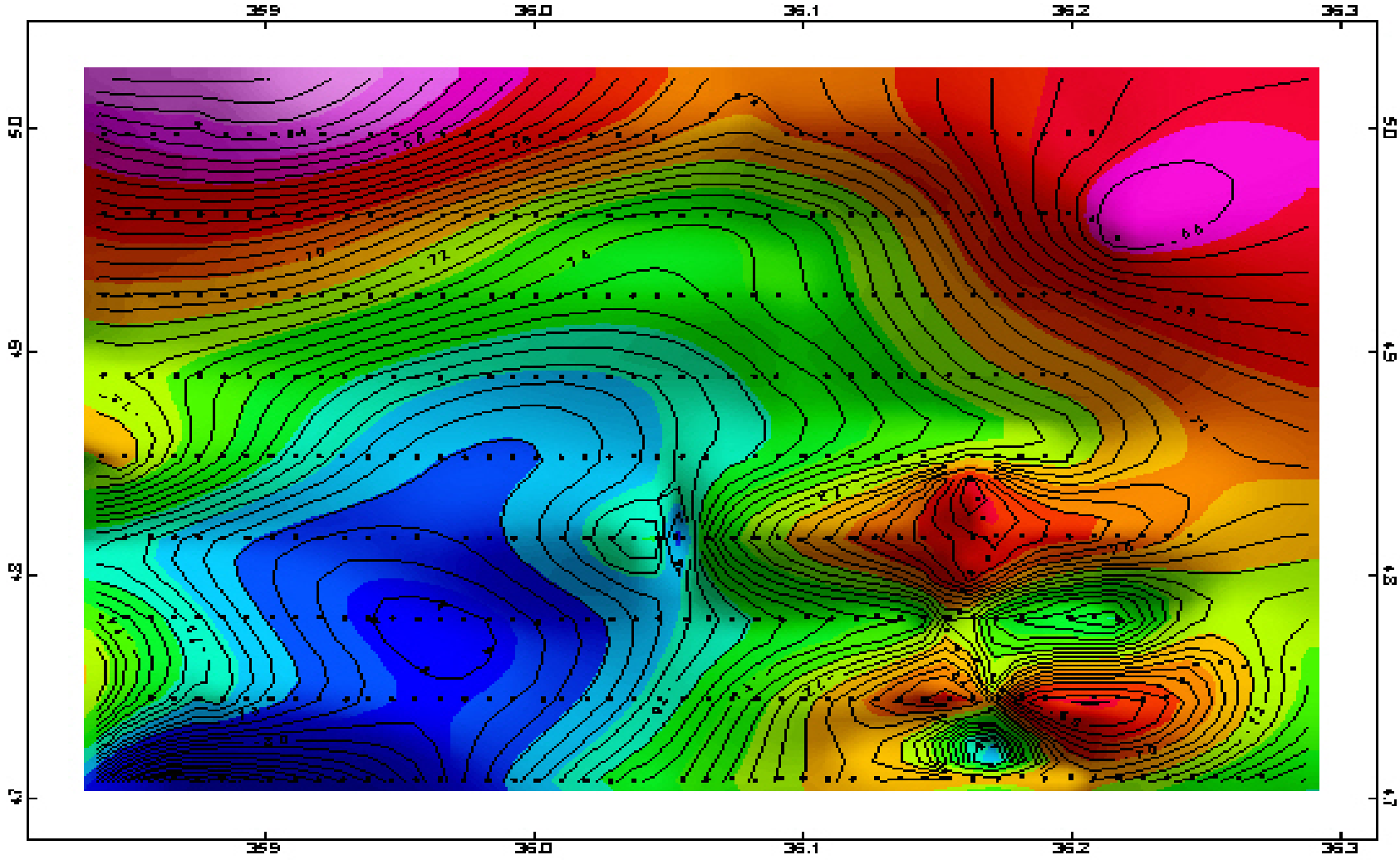

Fig.6- :LOWPASS FILTERED C_BOUGUER GRAVITY ANOMALY OF OMOB ASIN

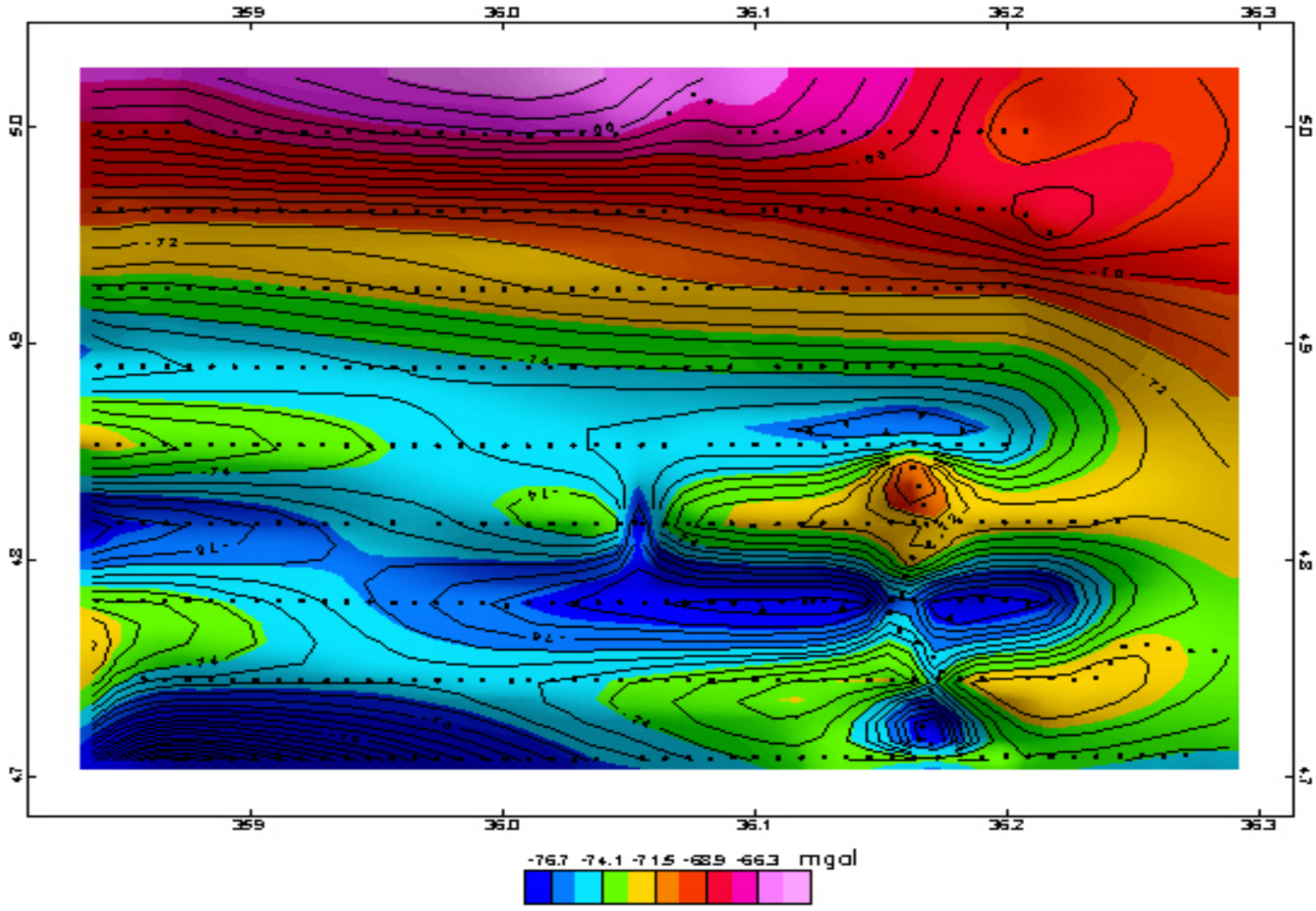

FIG.6- :RESIDUAL GRAVITY ANOMALY OF OMO BASIN

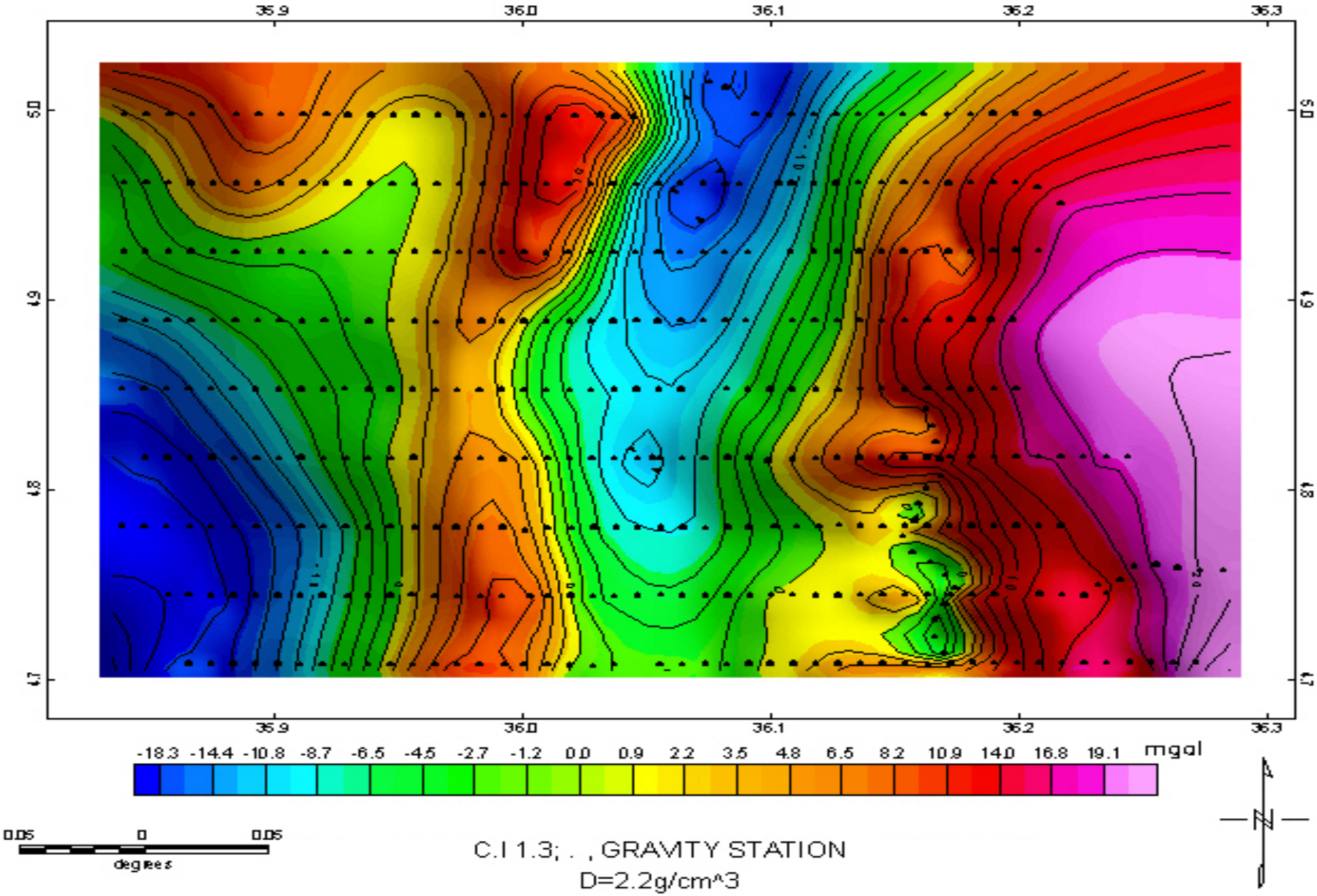

Fig.7.1:GRIDDED C- BOUGUR GRAVITY

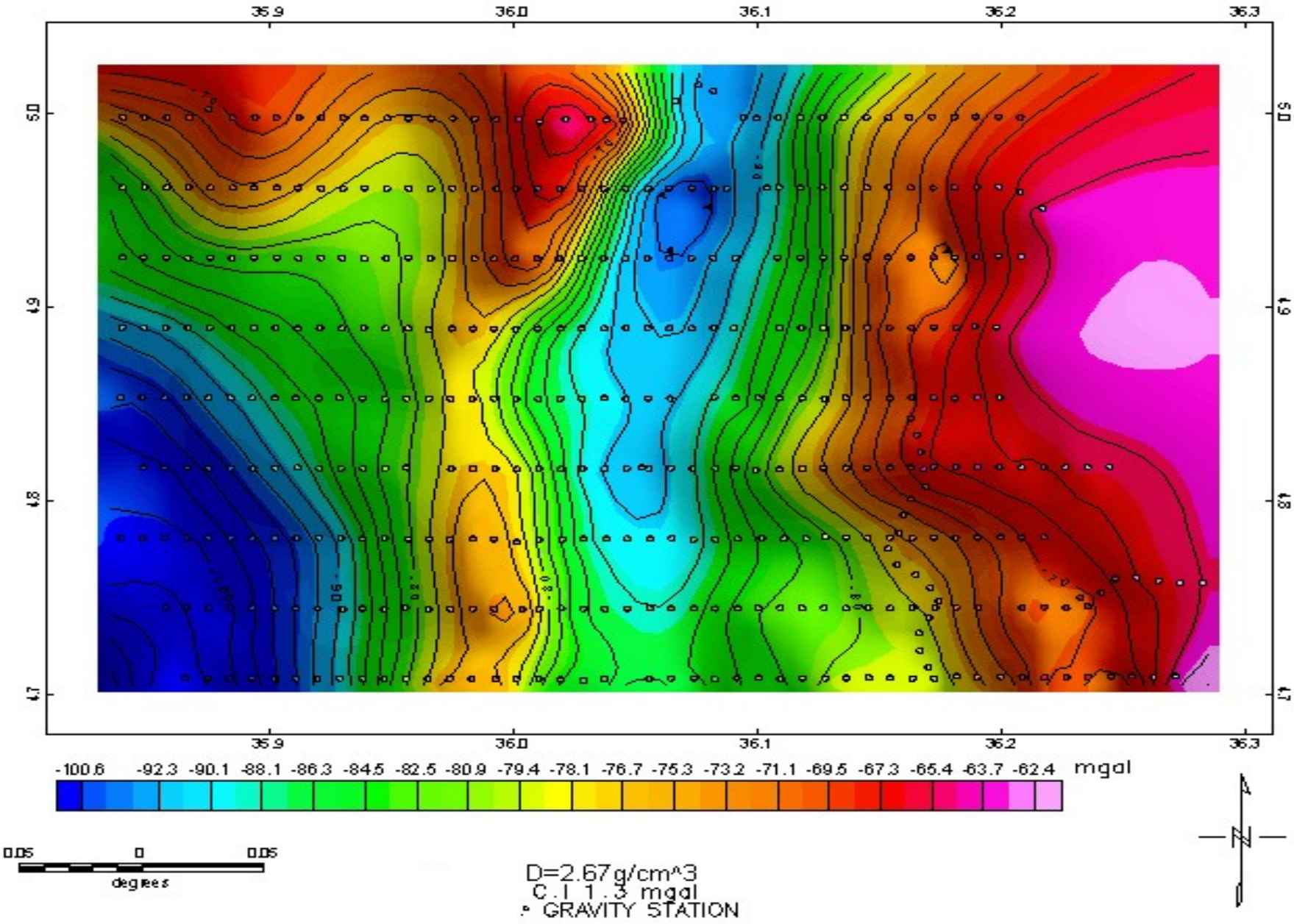

Fig.7.2:GRIDDED C- BOUGUR GRAVITY

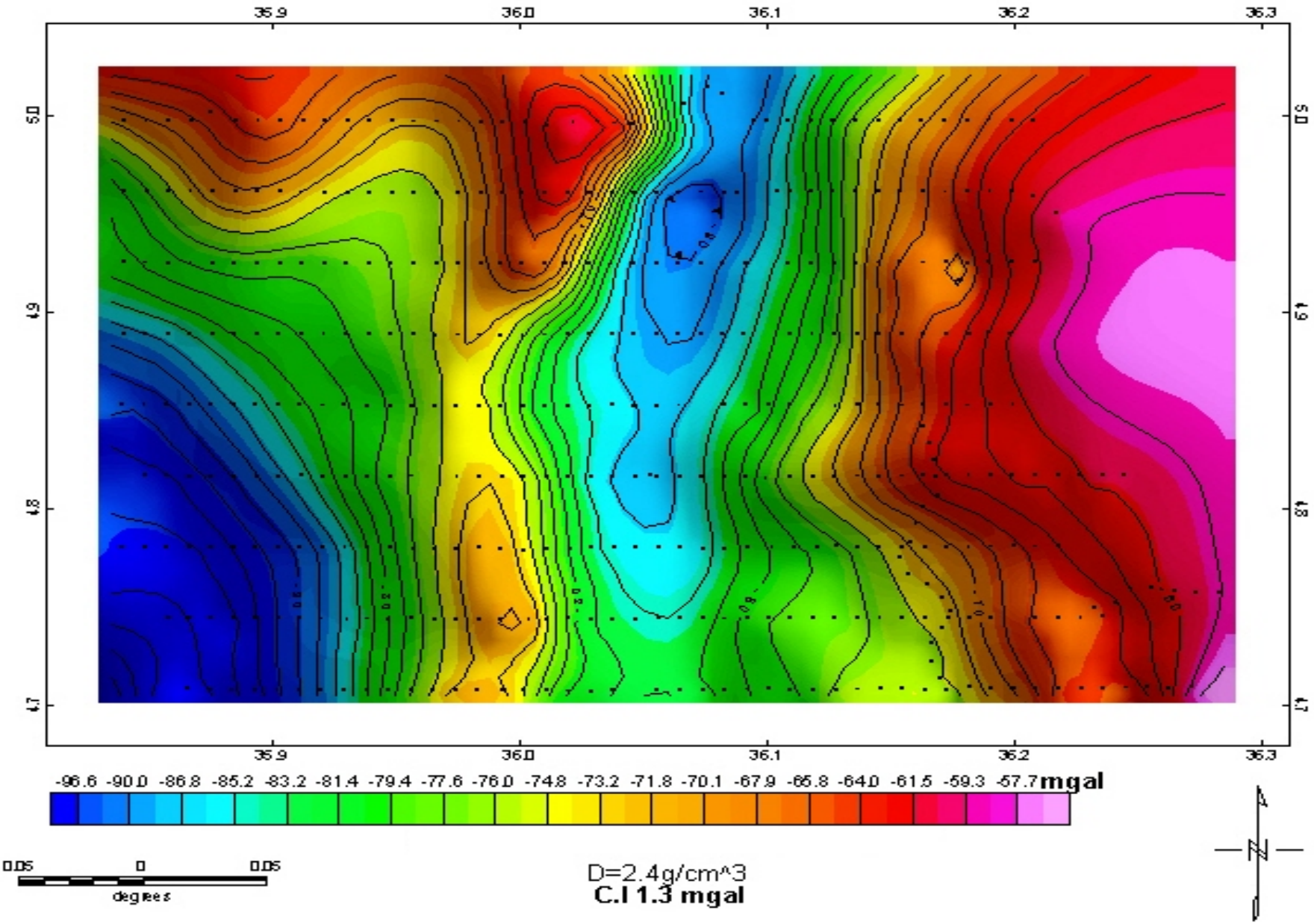

Fig.7.3:GRIDDED C- BOUGUR GRAVITY

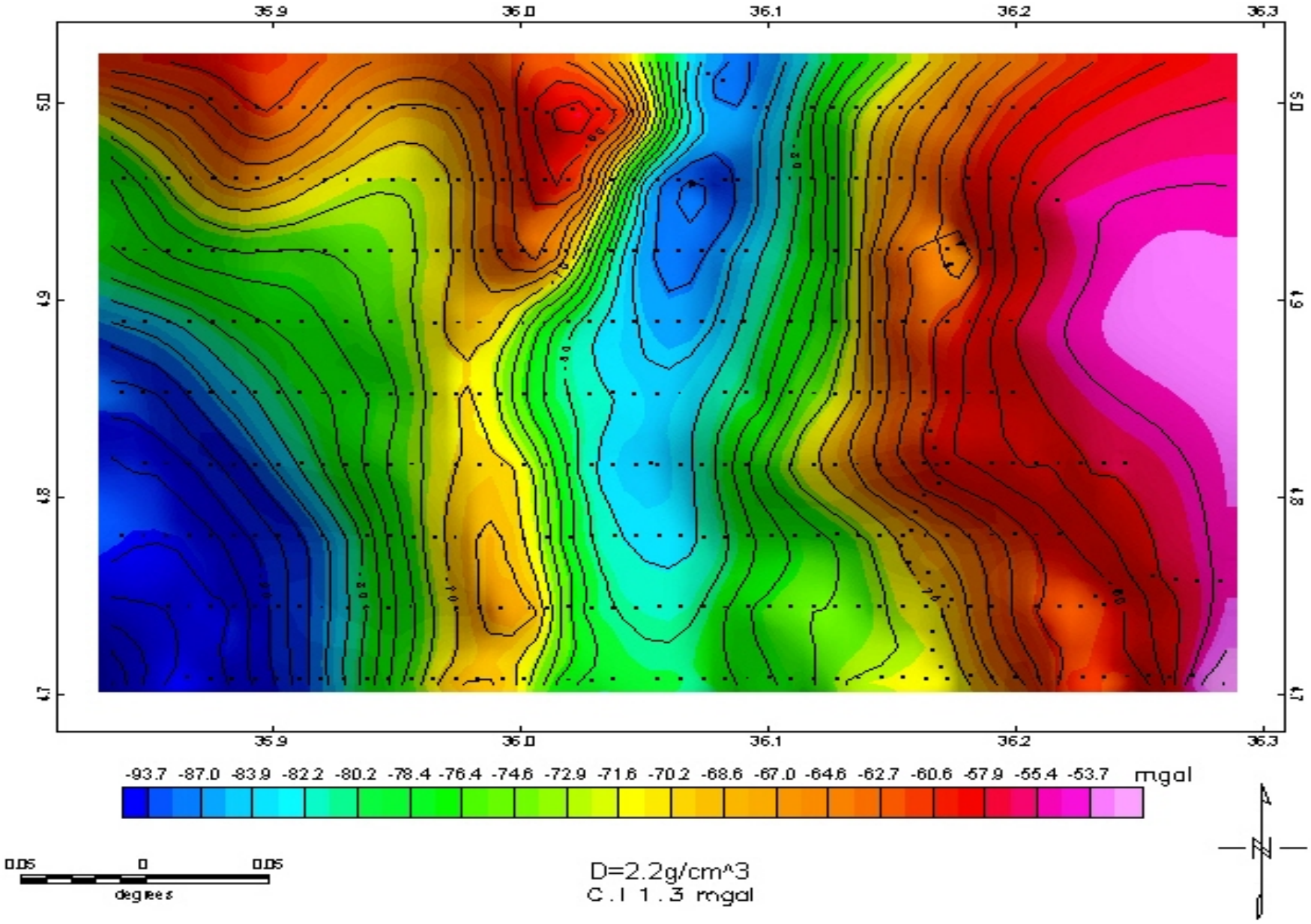

Fig.7.4: FIRST VERTICAL DERIVATIVE GRIDDED C- BOUGUR GRAVITY

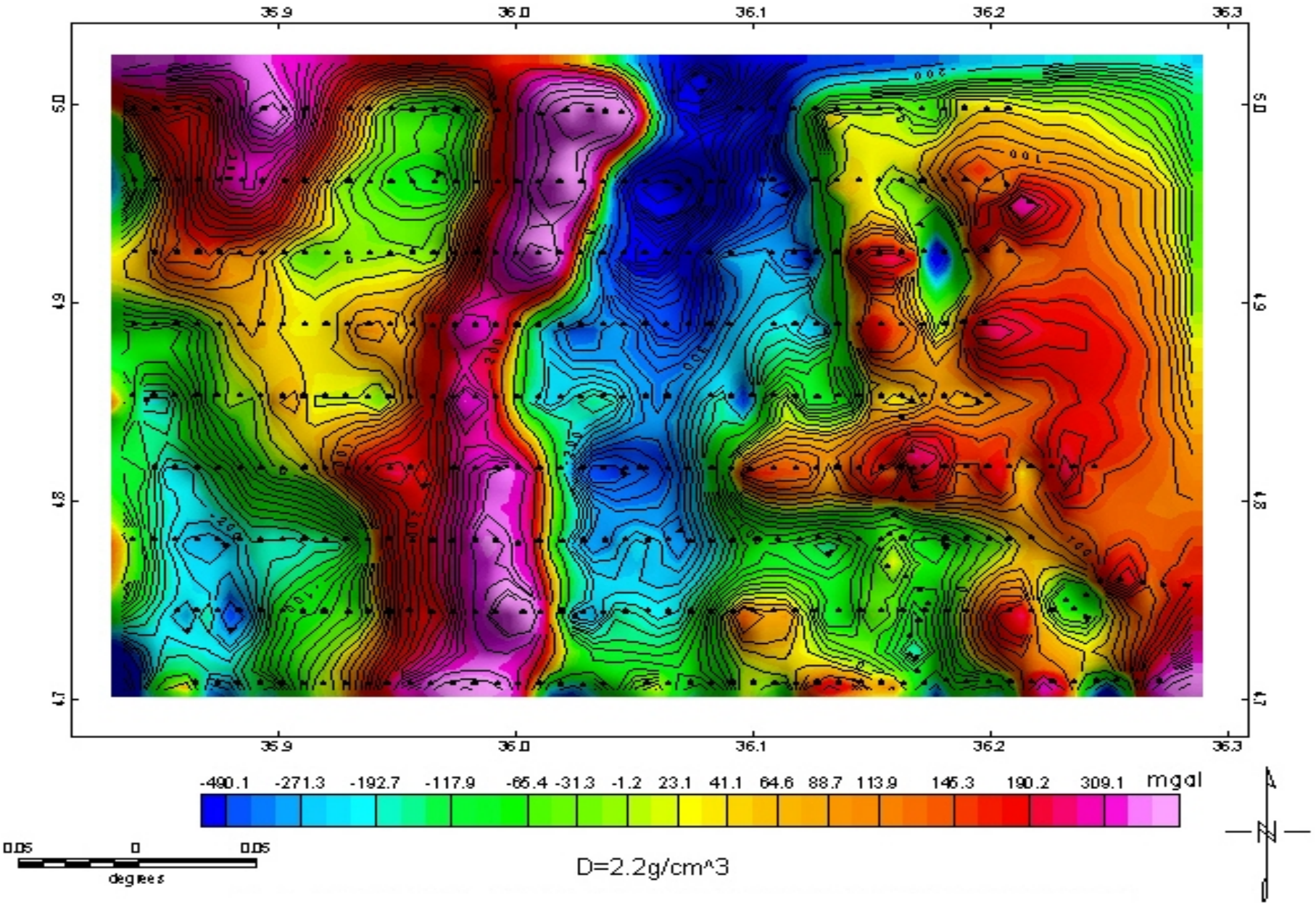

Fig.7.5: SECOND VERTICAL DERIVATIVE GRIDDED C- BOUGUR GRAVITY

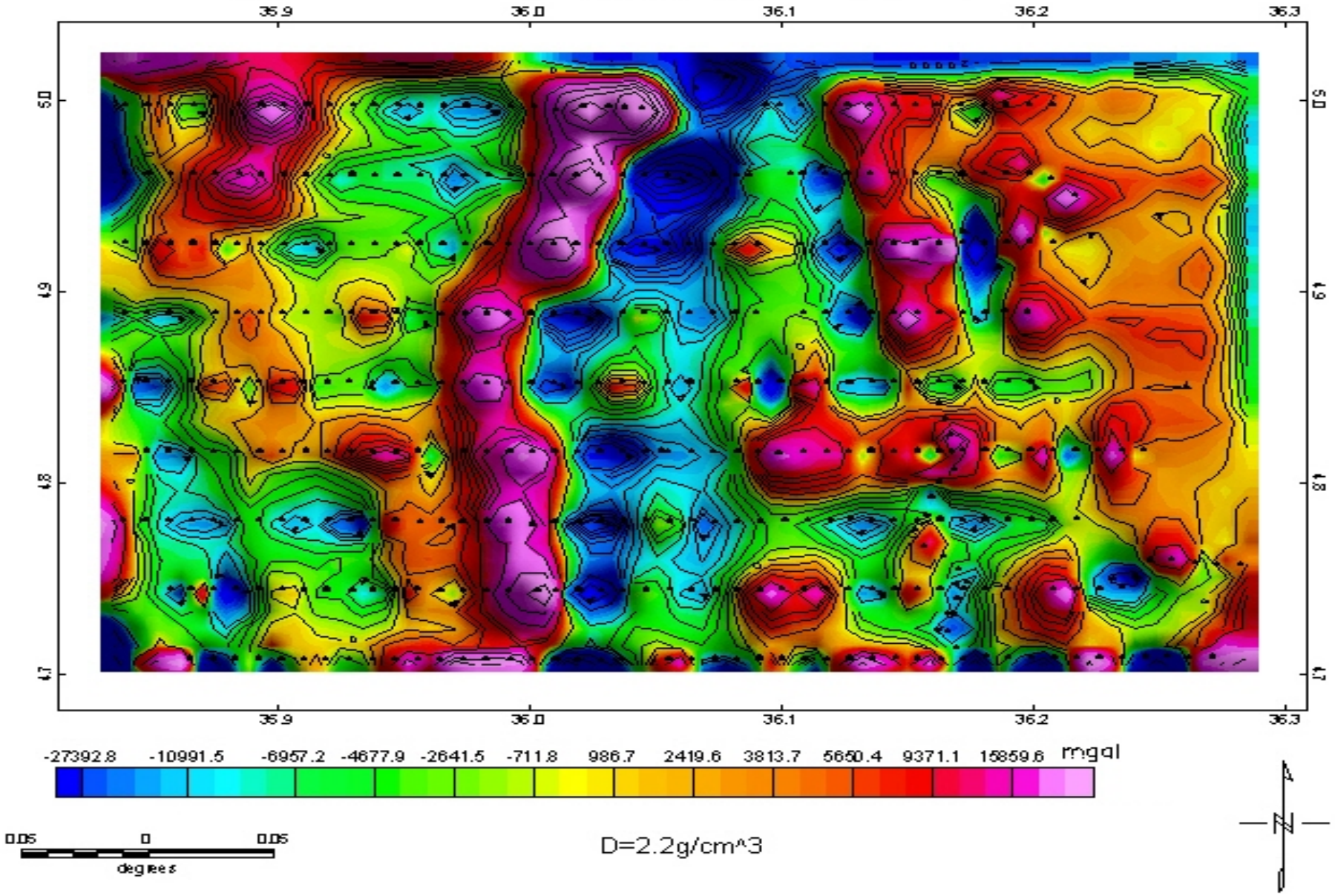

Fig : Residual 3D

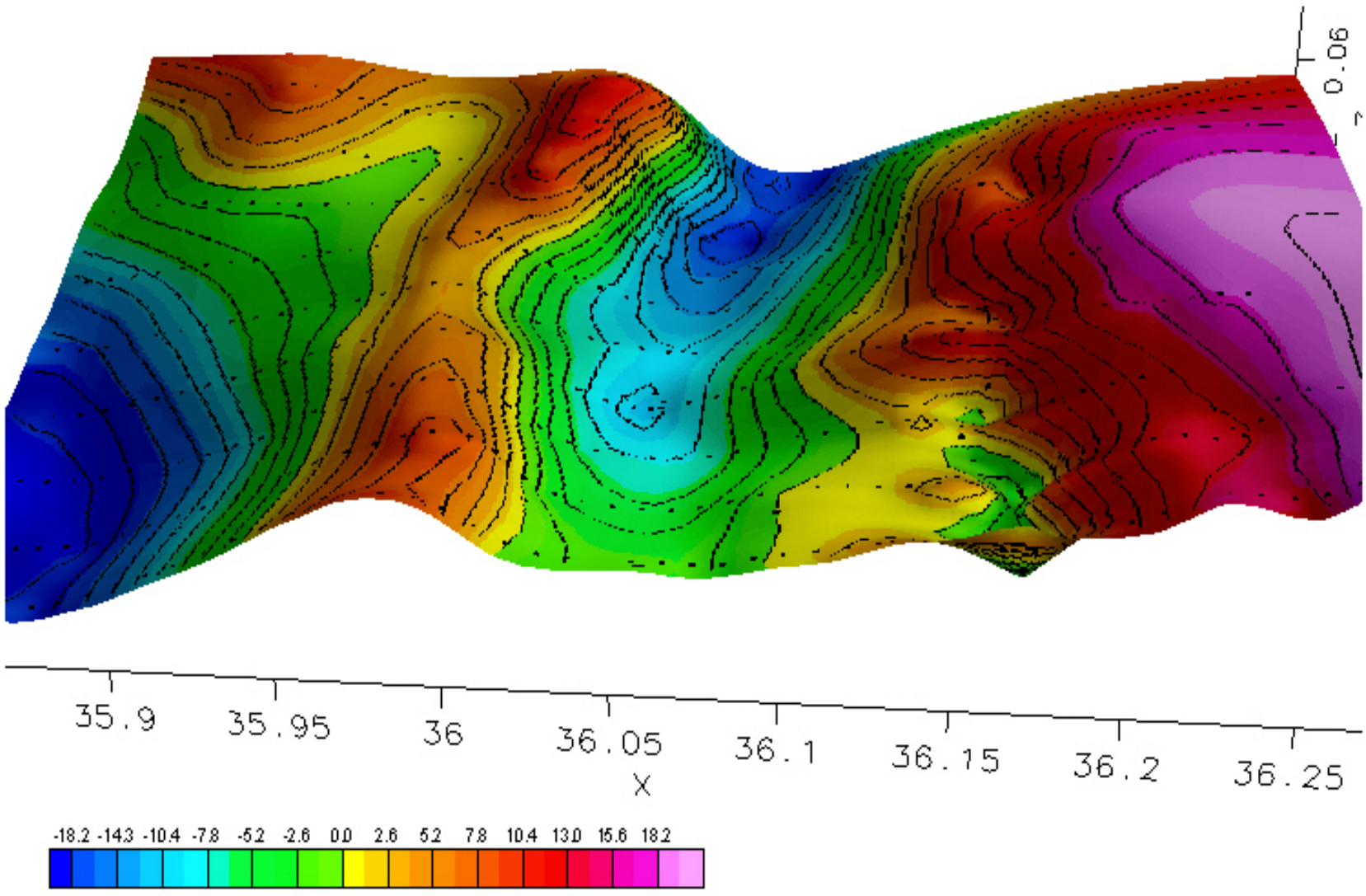

Fig.7.4: FIRST VERTICAL DERIVATIVE GRIDDED C. BOUGUR GRAVITY

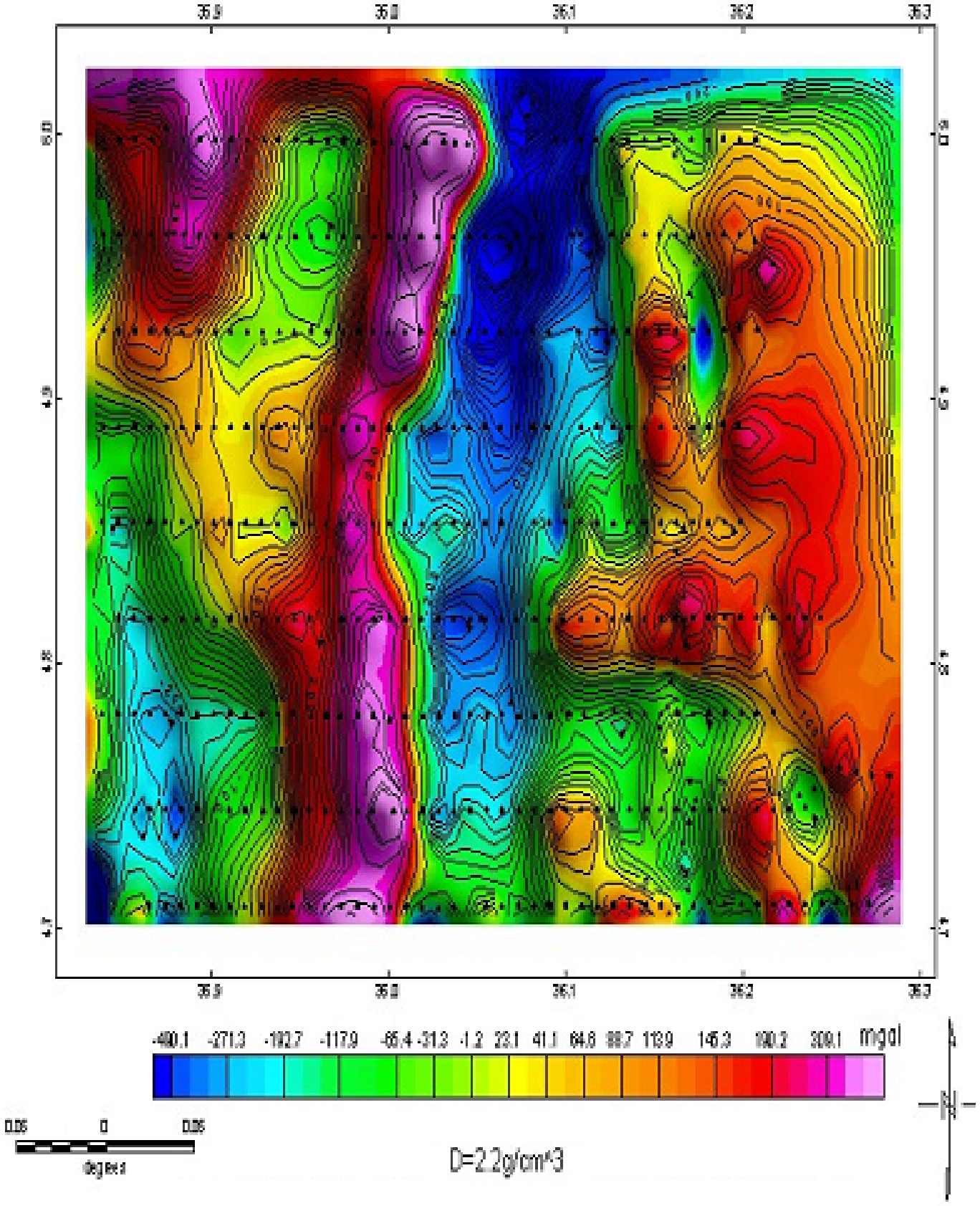

Fig.7.5: SECOND VERTICAL DERIVATIVE GRIDDED C. BOUGUR GRAVITY

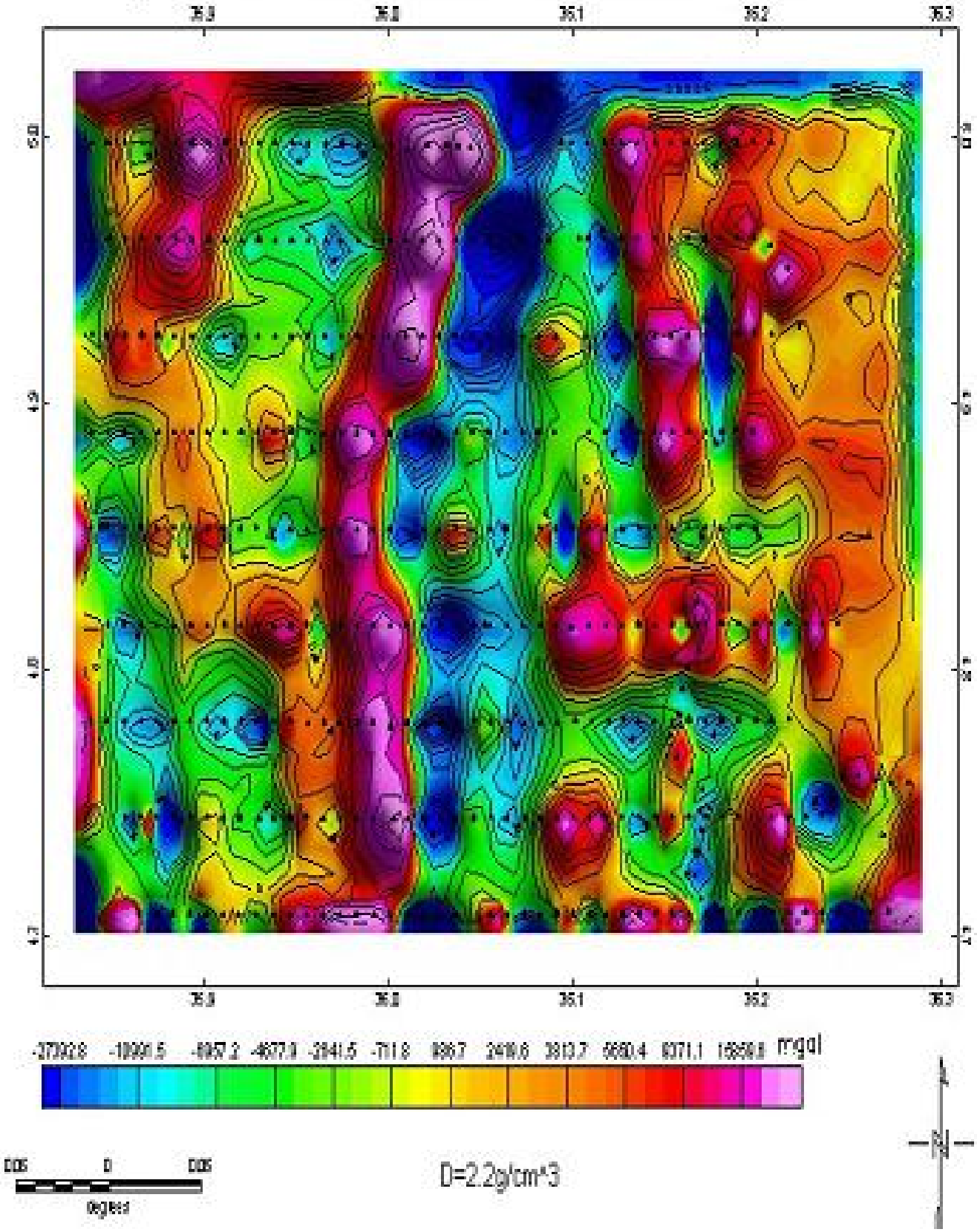

DECLARATION

I, the undersigned, hereby declare that this thesis is my original work carried out under the supervision of Dr. Tilahun Mamo and has not been presented as a thesis for a degree program in any other university, and that all sources of material used for the thesis have been duly acknowledged.

Solomon Salih

_____